



# TECH BRIEFS

NATIONAL AERONAUTICS AND SPACE ADMINISTRATION

-  **Technology Focus**
-  **Electronics/Computers**
-  **Software**
-  **Materials**
-  **Mechanics/Machinery**
-  **Manufacturing**
-  **Bio-Medical**
-  **Physical Sciences**
-  **Information Sciences**
-  **Books and Reports**
-  **Green Design**



# INTRODUCTION

Tech Briefs are short announcements of innovations originating from research and development activities of the National Aeronautics and Space Administration. They emphasize information considered likely to be transferable across industrial, regional, or disciplinary lines and are issued to encourage commercial application.

## Availability of NASA Tech Briefs and TSPs

Requests for individual Tech Briefs or for Technical Support Packages (TSPs) announced herein should be addressed to

### National Technology Transfer Center

Telephone No. (800) 678-6882 or via World Wide Web at [www.nttc.edu](http://www.nttc.edu)

Please reference the control numbers appearing at the end of each Tech Brief. Information on NASA's Innovative Partnerships Program (IPP), its documents, and services is also available at the same facility or on the World Wide Web at <http://www.nasa.gov/offices/ipp/network/index.html>

Innovative Partnerships Offices are located at NASA field centers to provide technology-transfer access to industrial users. Inquiries can be made by contacting NASA field centers listed below.

#### Ames Research Center

Mary Walsh  
(650) 604-1405  
[mary.w.walsh@nasa.gov](mailto:mary.w.walsh@nasa.gov)

#### Dryden Flight Research Center

Yvonne D. Gibbs  
(661) 276-3720  
[yvonne.d.gibbs@nasa.gov](mailto:yvonne.d.gibbs@nasa.gov)

#### Glenn Research Center

Joe Shaw, Acting Chief  
(216) 977-7135  
[robert.j.shaw@nasa.gov](mailto:robert.j.shaw@nasa.gov)

#### Goddard Space Flight Center

Nona Cheeks  
(301) 286-5810  
[nona.k.cheeks@nasa.gov](mailto:nona.k.cheeks@nasa.gov)

#### Jet Propulsion Laboratory

Indrani Graczyk  
(818) 354-2241  
[indrani.graczyk@jpl.nasa.gov](mailto:indrani.graczyk@jpl.nasa.gov)

#### Johnson Space Center

information  
(281) 483-3809  
[jsc.techtran@mail.nasa.gov](mailto:jsc.techtran@mail.nasa.gov)

#### Kennedy Space Center

David R. Makufka  
(321) 867-6227  
[david.r.makufka@nasa.gov](mailto:david.r.makufka@nasa.gov)

#### Langley Research Center

Elizabeth B. Plentovich  
(757) 864-2857  
[elizabeth.b.plentovich@nasa.gov](mailto:elizabeth.b.plentovich@nasa.gov)

#### Marshall Space Flight Center

Jim Dowdy  
(256) 544-7604  
[jim.dowdy@msfc.nasa.gov](mailto:jim.dowdy@msfc.nasa.gov)

#### Stennis Space Center

Ramona Travis  
(228) 688-3832  
[ramona.e.travis@nasa.gov](mailto:ramona.e.travis@nasa.gov)

#### Carl Ray, Program Executive

Small Business Innovation  
Research (SBIR) & Small  
Business Technology  
Transfer (STTR) Programs  
(202) 358-4652  
[carl.g.ray@nasa.gov](mailto:carl.g.ray@nasa.gov)

#### Doug Comstock, Partnerships

Innovation and Commercial  
Space Program Office (formerly IPP)  
(202) 358-2221  
[doug.comstock@nasa.gov](mailto:doug.comstock@nasa.gov)





# TECH BRIEFS

NATIONAL AERONAUTICS AND SPACE ADMINISTRATION



## 5 Technology Focus: Data Acquisition

- 5 Optimal Tuner Selection for Kalman-Filter-Based Aircraft Engine Performance Estimation
- 5 Airborne Radar Interferometric Repeat-Pass Processing
- 6 Plug-and-Play Environmental Monitoring Spacecraft Subsystem
- 7 Power-Combined GaN Amplifier With 2.28-W Output Power at 87 GHz



## 9 Software

- 9 Wallops Ship Surveillance System
- 9 Source Lines Counter (SLiC) Version 4.0
- 9 Guidance, Navigation, and Control Program
- 9 Single-Frame Terrain Mapping Software for Robotic Vehicles
- 10 Auto Draw From Excel Input Files
- 10 Observation Scheduling System
- 10 CFDP for Interplanetary Overlay Network
- 10 X-Windows Widget for Image Display



## 11 Electronics/Computers

- 11 Binary-Signal Recovery
- 11 Volumetric 3D Display System With Static Screen
- 12 MMIC Replacement for Gunn Diode Oscillators
- 12 Feature Acquisition With Imbalanced Training Data



## 13 Manufacturing & Prototyping

- 13 Mount Protects Thin-Walled Glass or Ceramic Tubes From Large Thermal and Vibration Loads
- 13 Carbon Nanotube-Based Structural Health Monitoring Sensors



## 15 Mechanics/Machinery

- 15 Wireless Inductive Power Device Suppresses Blade Vibrations
- 15 Safe, Advanced, Adaptable Isolation System Eliminates the Need for Critical Lifts
- 16 Anti-Rotation Device Releasable by Insertion of a Tool

- 16 A Magnetically Coupled Cryogenic Pump
- 17 Single Piezo-Actuator Rotary-Hammering Drill



## 19 Materials & Coatings

- 19 Fire-Retardant Polymeric Additives
- 19 Catalytic Generation of Lift Gases for Balloons
- 20 Ionic Liquids to Replace Hydrazine
- 21 Variable Emittance Electrochromics Using Ionic Electrolytes and Low Solar Absorptance Coatings



## 23 Green Design

- 23 Spacecraft Radiator Freeze Protection Using a Regenerative Heat Exchanger
- 23 Multi-Mission Power Analysis Tool



## 25 Physical Sciences

- 25 Correction for Self-Heating When Using Thermometers as Heaters in Precision Control Applications
- 25 Gravitational Wave Detection With Single-Laser Atom Interferometers
- 26 Titanium Alloy Strong Back for IXO Mirror Segments
- 26 Improved Ambient Pressure Pyroelectric Ion Source



## 29 Information Sciences

- 29 Multi-Modal Image Registration and Matching for Localization of a Balloon on Titan
- 29 Entanglement in Quantum-Classical Hybrid
- 29 Algorithm for Autonomous Landing
- 30 Quantum-Classical Hybrid for Information Processing
- 30 Small-Scale Dissipation in Binary-Species Transitional Mixing Layers
- 31 Superpixel-Augmented Endmember Detection for Hyperspectral Images
- 32 Coding for Parallel Links To Maximize the Expected Value of Decodable Messages



## 33 Bio-Medical

- 33 Microwave Tissue Soldering for Immediate Wound Closure

This document was prepared under the sponsorship of the National Aeronautics and Space Administration. Neither the United States Government nor any person acting on behalf of the United States Government assumes any liability resulting from the use of the information contained in this document, or warrants that such use will be free from privately owned rights.





### ➤ **Optimal Tuner Selection for Kalman-Filter-Based Aircraft Engine Performance Estimation**

**The new methodology reduces parameter estimation errors by more than 50 percent.**

*John H. Glenn Research Center, Cleveland, Ohio*

An emerging approach in the field of aircraft engine controls and system health management is the inclusion of real-time, onboard models for the in-flight estimation of engine performance variations. This technology, typically based on Kalman-filter concepts, enables the estimation of unmeasured engine performance parameters that can be directly utilized by controls, prognostics, and health-management applications. A challenge that complicates this practice is the fact that an aircraft engine's performance is affected by its level of degradation, generally described in terms of unmeasurable health parameters such as efficiencies and flow capacities related to each major engine module. Through Kalman-filter-based estimation techniques, the level of engine performance degradation can be estimated, given that there are at least as many sensors as health parameters to be estimated. However, in an aircraft engine, the number of sensors available is typically less than the number of health parameters, presenting an under-determined estimation problem. A common

approach to address this shortcoming is to estimate a subset of the health parameters, referred to as model tuning parameters. The problem/objective is to optimally select the model tuning parameters to minimize Kalman-filter-based estimation error.

A tuner selection technique has been developed that specifically addresses the under-determined estimation problem, where there are more unknown parameters than available sensor measurements. A systematic approach is applied to produce a model tuning parameter vector of appropriate dimension to enable estimation by a Kalman filter, while minimizing the estimation error in the parameters of interest. Tuning parameter selection is performed using a multi-variable iterative search routine that seeks to minimize the theoretical mean-squared estimation error of the Kalman filter. This approach can significantly reduce the error in onboard aircraft engine parameter estimation applications such as model-based diagnostic, controls, and life usage calculations.

The advantage of the innovation is the significant reduction in estimation errors that it can provide relative to the conventional approach of selecting a subset of health parameters to serve as the model tuning parameter vector. Because this technique needs only to be performed during the system design process, it places no additional computation burden on the onboard Kalman filter implementation.

The technique has been developed for aircraft engine onboard estimation applications, as this application typically presents an under-determined estimation problem. However, this generic technique could be applied to other industries using gas turbine engine technology.

*This work was done by Donald L. Simon and Sanjay Garg of Glenn Research Center. Further information is contained in a TSP (see page 1).*

*Inquiries concerning rights for the commercial use of this invention should be addressed to NASA Glenn Research Center, Innovative Partnerships Office, Attn: Steve Fedor, Mail Stop 4-8, 21000 Brookpark Road, Cleveland, Ohio 44135. Refer to LEW-18458-1.*

### ➤ **Airborne Radar Interferometric Repeat-Pass Processing**

**Improvements have resolved some of the earlier difficulties.**

*NASA's Jet Propulsion Laboratory, Pasadena, California*

Earth science research often requires crustal deformation measurements at a variety of time scales, from seconds to decades. Although satellites have been used for repeat-track interferometric (RTI) synthetic-aperture-radar (SAR) mapping for close to 20 years, RTI is much more difficult to implement from an airborne platform owing to the irregular trajectory of the aircraft compared with microwave imaging radar wavelengths. Two basic requirements for robust airborne repeat-pass radar interferometry include the ability to fly the

platform to a desired trajectory within a narrow tube and the ability to have the radar beam pointed in a desired direction to a fraction of a beam width. Uninhabited Aerial Vehicle Synthetic Aperture Radar (UAVSAR) is equipped with a precision auto pilot developed by NASA Dryden that allows the platform, a Gulfstream III, to nominally fly within a 5 m diameter tube and with an electronically scanned antenna to position the radar beam to a fraction of a beam width based on INU (inertial navigation unit) attitude angle measurements.

UAVSAR is also equipped with a set of GPS receivers that coupled with INU measurements are used to determine the antenna position to a high degree of accuracy on a pulse-to-pulse basis. The relative position error within a flight track is measured to a small fraction of a wavelength as is required for image formation; however, the absolute accuracy of the position measurements is in the 2-10 cm range limited by the accuracy of post flight processed differential GPS data. In order to make repeat-pass radar interferometric deformation maps suit-

able for geophysical interpretation, the relative position between the platform positions at the time a point is imaged for a pair of repeat-pass observations, i.e. the interferometric baseline, needs to be known to the millimeter level. Bridging the gap from the 2–10 cm position accuracy of the metrology system to the desired millimeter relative position accuracy uses information contained within the SAR imagery. Image-based residual motion recovery algorithms using radar imagery have been developed for airborne (and spaceborne) platforms previously; however, these algorithms have not been employed for systems using electronically scanned arrays.

The UAVSAR repeat-pass processing software called JPRP, has been specifically designed to permit the generation of radar repeat-pass interferograms of surface deformation suitable for geophysical

interpretation. This software automatically processes and co-registers data from multiple flight lines. JPRP has been modified from previous codes to do motion compensation and image formation for airborne systems employing electronically scanned antennas. Since UAVSAR employs an onboard Block Floating Point Quantization (BFPQ) scheme whereby 12 bit recorded radar echoes can be compressed to  $M$  bits where  $M$  ranges from 2–10 and is a radar commandable parameter, the JPRP includes appropriate BFPQ decoding algorithms. JPRP also includes code and algorithms for computing the repeat-pass interferometric baselines for airborne data using *a priori* GPS and INU data and for estimating refined residual baselines from the radar imagery needed for resolving dynamic residual baselines at the subcentimeter level. These algorithms have been adapted to work for systems

employing electronically scanned antennas. The program includes advanced repeat-pass motion compensation algorithms that include subaperture, terrain-dependent motion compensation for range/Doppler, or wave domain processing. Also, a new algorithm that is computationally efficient was developed for topographic fringe removal and geolocation.

*This work was done by Scott Hensley, Thierry R. Michel, Cathleen E. Jones, Ronald J. Muellerschoen, Bruce D. Chapman, Alexander Fore, and Marc Simard of Caltech and Howard A. Zebker of Stanford University for NASA's Jet Propulsion Laboratory. For more information, contact iaoffice@jpl.nasa.gov.*

*The software used in this innovation is available for commercial licensing. Please contact Daniel Broderick of the California Institute of Technology at danielb@caltech.edu. Refer to NPO-46093.*

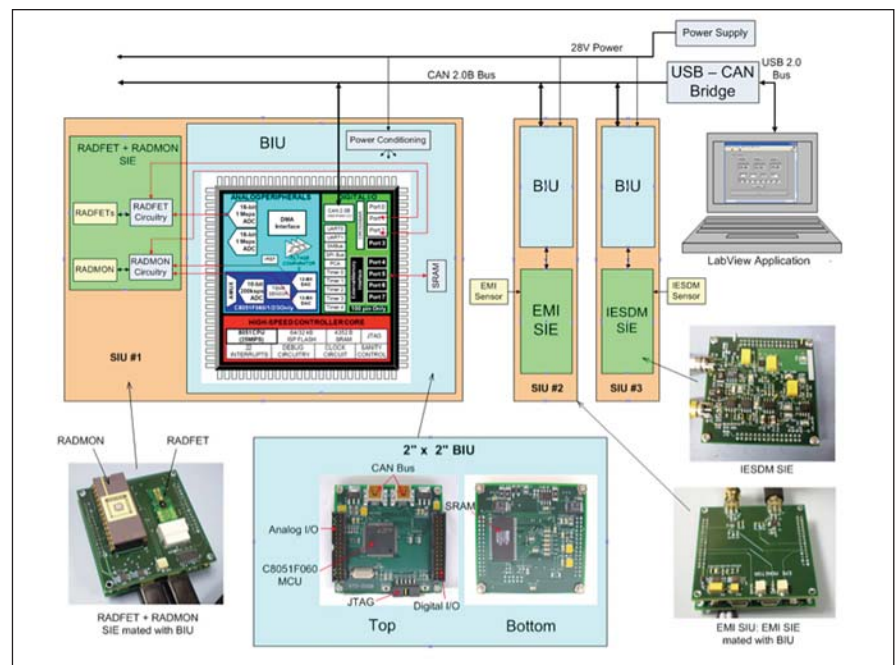
## Plug-and-Play Environmental Monitoring Spacecraft Subsystem

**New architecture provides real-time information to validating spacecraft health in harsh environments.**

*NASA's Jet Propulsion Laboratory, Pasadena, California*

A Space Environment Monitor (SEM) subsystem architecture has been developed and demonstrated that can benefit future spacecraft by providing (1) real-time knowledge of the spacecraft state in terms of exposure to the environment; (2) critical, instantaneous information for anomaly resolution; and (3) invaluable environmental data for designing future missions. The SEM architecture consists of a network of plug-and-play (PnP) Sensor Interface Units (SIUs), each servicing one or more environmental sensors. The SEM architecture is influenced by the IEEE Smart Transducer Interface Bus standard (IEEE Std 1451) for its PnP functionality. A network of PnP Spacecraft SIUs is enabling technology for gathering continuous real-time information critical to validating spacecraft health in harsh space environments.

The demonstrated system that provided a proof-of-concept of the SEM architecture consisted of three SIUs for measurement of total ionizing dose (TID) and single event upset (SEU) radiation effects, electromagnetic interference (EMI), and deep dielectric charging through use of a prototype Internal Electro-Static Discharge Monitor (IESDM). Each SIU consists of two



**Space Environment Monitor Demonstration System.**

stacked 2×2 in. (≈5×5 cm) circuit boards: a Bus Interface Unit (BIU) board that provides data conversion, processing and connection to the SEM power-and-data bus, and a Sensor Interface Electronics (SIE) board that provides sensor

interface needs and data path connection to the BIU. The figure illustrates the demonstration system components and connectivity where SIU #1 functions as a radiation monitor, servicing a Radiation Field Effect Transistor (RADFET)

TID sensor and a RADiation MONitor (RADMON) SEU sensor, SIU #2 monitors EMI through use of two RF antenna, and SIU #3 monitors spacecraft charging conditions by interfacing to an IESDM sensor. The heart of the BIU is a Silicon Laboratories C8051F060, a mixed-signal in-circuit-programmable

(ISP) flash micro controller unit (MCU) with controller-area network (CAN) bus interface.

At the time of this reporting, follow-on work is needed to develop designs that use space-qualified parts, in developing a standard fault-tolerant spacecraft interface, which would spawn a

multidrop backbone SIU bus (i.e. CAN), and in developing the PnP software that leverages off IEEE Std 1451.

*This work was done by Jagdish Patel, David E. Brinza, Tuan A. Tran, and Brent R. Blaes of Caltech for NASA's Jet Propulsion Laboratory. Further information is contained in a TSP (see page 1). NPO-47340*

## ➤ Power-Combined GaN Amplifier With 2.28-W Output Power at 87 GHz

**Applications include radar and remote sensing spectrometers, and W-band communications.**

*NASA's Jet Propulsion Laboratory, Pasadena, California*

Future remote sensing instruments will require focal plane spectrometer arrays with higher resolution at high frequencies. One of the major components of spectrometers are the local oscillator (LO) signal sources that are used to drive mixers to down-convert received radio-frequency (RF) signals to intermediate frequencies (IFs) for analysis. By advancing LO technology through increasing output power and efficiency, and reducing component size, these advances will improve performance and simplify architecture of spectrometer array systems. W-band power amplifiers (PAs) are an essential element of current frequency-multiplied submillimeter-wave LO signal sources. Substantial W-band (75–110 GHz) power is required due to the lossy passive frequency multipliers used to generate higher frequency

signals in nonlinear Schottky diode based LO sources. By advancing PA technology, the LO system performance can be increased with possible cost reductions compared to current gallium arsenide (GaAs) PA technology.

This work utilizes GaN monolithic millimeter-wave integrated circuit (MMIC) PAs developed from a new HRL Laboratories LLC 0.15- $\mu\text{m}$  gate length GaN semiconductor transistor. By additionally waveguide power combining PA MMIC modules, the researchers here target the highest output power performance and efficiency in the smallest volume achievable for W-band. GaN has higher voltage breakdown capability than other currently available W-band semiconductor technology such as GaAs. GaN PAs have shown significant improvements compared to state-of-the-

art GaAs PAs in W-band for output power density and efficiency.

High-power, high-efficiency GaN PAs are cross-cutting and can enable more efficient LO distribution systems for new astrophysics and planetary receivers and heterodyne array instruments. They can also allow for a new electronically scannable solid-state array technology for future Earth science radar instruments and communication platforms.

*This work was done by King Man Fung, John Ward, Goutam Chattopadhyay, Robert H. Lin, Lorene A. Samoska, Pekka P. Kangaslahti, Imran Mehdi, Bjorn H. Lambriksen, Paul F. Goldsmith, Mary M. Soria, Joelle T. Cooperrider, and Peter J. Bruneau of Caltech; and Ara Kurdoghlian and Miroslav Miroslav of HRL Laboratories for NASA's Jet Propulsion Laboratory. For more information, contact [iaoffice@jpl.nasa.gov](mailto:iaoffice@jpl.nasa.gov). NPO-47450*





## Wallops Ship Surveillance System

Approved as a Wallops control center backup system, the Wallops Ship Surveillance Software is a day-of-launch risk analysis tool for spaceport activities. The system calculates impact probabilities and displays ship locations relative to boundary lines. It enables rapid analysis of possible flight paths to preclude the need to cancel launches and allow execution of launches in a timely manner. Its design is based on low-cost, large-customer-base elements including personal computers, the Windows operating system, C/C++ object-oriented software, and network interfaces. In conformance with the NASA software safety standard, the system is designed to ensure that it does not falsely report a safe-for-launch condition. To improve the current ship surveillance method, the system is designed to prevent delay of launch under a safe-for-launch condition.

A single workstation is designated the controller of the official ship information and the official risk analysis. Copies of this information are shared with other networked workstations. The program design is divided into five subsystems areas:

1. Communication Link – threads that control the networking of workstations;
2. Contact List – a thread that controls a list of protected item (ocean vessel) information;
3. Hazard List – threads that control a list of hazardous item (debris) information and associated risk calculation information;
4. Display – threads that control operator inputs and screen display outputs; and
5. Archive – a thread that controls archive file read and write access.

Currently, most of the hazard list thread and parts of other threads are being reused as part of a new ship surveillance system, under the SureTrak project.

*This work was done by Donna C. Smith of Goddard Space Flight Center. Further information is contained in a TSP (see page 1). GSC-15623-1*

## Source Lines Counter (SLiC) Version 4.0

Source Lines Counter (SLiC) is a software utility designed to measure software source code size using logical

source statements and other common measures for 22 of the programming languages commonly used at NASA and the aerospace industry. Such metrics can be used in a wide variety of applications, from parametric cost estimation to software defect analysis. SLiC has a variety of unique features such as automatic code search, automatic file detection, hierarchical directory totals, and spreadsheet-compatible output. SLiC was written for extensibility; new programming language support can be added with minimal effort in a short amount of time. SLiC runs on a variety of platforms including UNIX, Windows, and Mac OSX. Its straightforward command-line interface allows for customization and incorporation into the software build process for tracking development metrics.

*This work was done by Erik W. Monson, Kevin A. Smith, Brian J. Newport, Roli D. Gostelow, Jairus M. Hihn, and Ronald K. Kandt of Caltech for NASA's Jet Propulsion Laboratory. For more information, contact iaoffice@jpl.nasa.gov.*

*This software is available for commercial licensing. Please contact Daniel Broderick of the California Institute of Technology at danielb@caltech.edu. Refer to NPO-45962.*

## Guidance, Navigation, and Control Program

The Rendezvous and Proximity Operations Program (RPOP) is real-time guidance, navigation, and control (GN&C) domain piloting-aid software that provides 3D Orbiter graphics and runs on the Space Shuttle's Criticality-3 Payload and General Support Computer (PGSC) in the crew cockpit. This software provides the crew with "Situational Awareness" during the rendezvous and proximity operations phases of flight. RPOP can be configured from flight to flight, accounting for mission-specific flight scenarios and target vehicles, via initialization load (I-load) data files. The software provides real-time, automated, closed-loop guidance recommendations and the capability to integrate the crew's manual backup techniques.

The software can bring all relative navigation sensor data, including the Orbiter's GPC (general purpose computer) data, into one central application to provide comprehensive situational

awareness of the rendezvous and proximity operations trajectory.

RPOP also can separately maintain trajectory estimates (past, current, and predicted) based on certain data types and co-plot them, in order to show how the various navigation solutions compare. RPOP's best estimate of the relative trajectory is determined by a relative Kalman filter processing data provided by the sensor suite's most accurate sensor, the trajectory control sensor (TCS). Integrated with the Kalman filter is an algorithm that identifies the reflector that the TCS is tracking.

Because RPOP runs on PC laptop computers, the development and certification lifecycles are more agile, flexible, and cheaper than those that govern the Orbiter FSW (flight software) that runs in the GPC. New releases of RPOP can be turned around on a 3- to 6-month template, from new Change Request (CR) to certification, depending on the complexity of the changes.

*This work was done by Heather Hinkel, Scott Tamblin, and William L. Jackson of NASA's Johnson Space Center; Chris Foster of Jacobs Engineering (ESCG); Jack Brazzel and Thomas R. Manning of McDonnell Douglas Space Systems; and Fred Clark, Pete Shepar, Jim D. Barrett, and Zoran Milenkovic of Lockheed Martin. Further information is contained in a TSP (see page 1). MSC-24473-1*

## Single-Frame Terrain Mapping Software for Robotic Vehicles

This software is a component in an unmanned ground vehicle (UGV) perception system that builds compact, single-frame terrain maps for distribution to other systems, such as a world model or an operator control unit, over a local area network (LAN). Each cell in the map encodes an elevation value, terrain classification, object classification, terrain traversability, terrain roughness, and a confidence value into four bytes of memory. The input to this software component is a range image (from a lidar or stereo vision system), and optionally a terrain classification image and an object classification image, both registered to the range image. The single-frame terrain map generates estimates of the support surface elevation, ground cover elevation, and minimum canopy elevation; gener-

ates terrain traversability cost; detects low overhangs and high-density obstacles; and can perform geometry-based terrain classification (ground, ground cover, unknown).

A new origin is automatically selected for each single-frame terrain map in global coordinates such that it coincides with the corner of a world map cell. That way, single-frame terrain maps correctly line up with the world map, facilitating the merging of map data into the world map. Instead of using 32 bits to store the floating-point elevation for a map cell, the vehicle elevation is assigned to the map origin elevation and reports the change in elevation (from the origin elevation) in terms of the number of discrete steps. The single-frame terrain map elevation resolution is 2 cm. At that resolution, terrain elevation from -20.5 to 20.5 m (with respect to the vehicle's elevation) is encoded into 11 bits.

For each four-byte map cell, bits are assigned to encode elevation, terrain roughness, terrain classification, object classification, terrain traversability cost, and a confidence value. The vehicle's current position and orientation, the map origin, and the map cell resolution are all included in a header for each map. The map is compressed into a vector prior to delivery to another system.

*This work was done by Arturo L. Rankin of Caltech for NASA's Jet Propulsion Laboratory. Further information is contained in a TSP (see page 1).*

*This software is available for commercial licensing. Please contact Daniel Broderick of the California Institute of Technology at [danielb@caltech.edu](mailto:danielb@caltech.edu). Refer to NPO-47039.*

## Auto Draw From Excel Input Files

The design process often involves the use of Excel files during project development. To facilitate communications of the information in the Excel files, drawings are often generated. During the design process, the Excel files are updated often to reflect new input. The problem is that the drawings often lag the updates, often leading to confusion of the current state of the design.

The use of this program allows visualization of complex data in a format that is more easily understandable than pages of numbers. Because the graphical output can be updated automatically, the manual labor of diagram drawing can be eliminated. The more frequent update of system diagrams can reduce confusion and reduce errors and is likely

to uncover symmetric problems earlier in the design cycle, thus reducing rework and redesign.

*This work was done by Karl F. Strauss, Renaud Goullioud, Brian Cox, and James M. Grimes of Caltech for NASA's Jet Propulsion Laboratory. For more information, contact [iaoffice@jpl.nasa.gov](mailto:iaoffice@jpl.nasa.gov).*

*This software is available for commercial licensing. Please contact Daniel Broderick of the California Institute of Technology at [danielb@caltech.edu](mailto:danielb@caltech.edu). Refer to NPO-46926.*

## Observation Scheduling System

Software has been designed to schedule remote sensing with the Earth Observing One spacecraft. The software attempts to satisfy as many observation requests as possible considering each against spacecraft operation constraints such as data volume, thermal, pointing maneuvers, and others. More complex constraints such as temperature are approximated to enable efficient reasoning while keeping the spacecraft within safe limits. Other constraints are checked using an external software library. For example, an attitude control library is used to determine the feasibility of maneuvering between pairs of observations. This innovation can deal with a wide range of spacecraft constraints and solve large scale scheduling problems like hundreds of observations and thousands of combinations of observation sequences.

*This work was done by Steve A. Chien, Daniel Q. Tran, Gregg R. Rabideau, and Steven R. Schaffer of Caltech for NASA's Jet Propulsion Laboratory. For more information, contact [iaoffice@jpl.nasa.gov](mailto:iaoffice@jpl.nasa.gov).*

*This software is available for commercial licensing. Please contact Daniel Broderick of the California Institute of Technology at [danielb@caltech.edu](mailto:danielb@caltech.edu). Refer to NPO-47189.*

## CFDP for Interplanetary Overlay Network

The CCSDS (Consultative Committee for Space Data Systems) File Delivery Protocol for Interplanetary Overlay Network (CFDP-ION) is an implementation of CFDP that uses ION's DTN (delay tolerant networking) implementation as its UT (unit-data transfer) layer. Because the DTN protocols effect automatic, reliable transmission via multiple relays, CFDP-ION need only satisfy the requirements for Class 1 ("unacknowledged") CFDP. This keeps the implementation small, but without loss of capability.

This innovation minimizes processing resources by using zero-copy objects for file data transmission. It runs without modification in VxWorks, Linux, Solaris, and OS/X. As such, this innovation can be used without modification in both flight and ground systems. Integration with DTN enables the CFDP implementation itself to be very simple; therefore, very small. Use of ION infrastructure minimizes consumption of storage and processing resources while maximizing safety.

*This work was done by Scott C. Burleigh of Caltech for NASA's Jet Propulsion Laboratory. Further information is contained in a TSP (see page 1).*

*The software used in this innovation is available for commercial licensing. Please contact Daniel Broderick of the California Institute of Technology at [danielb@caltech.edu](mailto:danielb@caltech.edu). Refer to NPO-47084.*

## X-Windows Widget for Image Display

XvicImage is a high-performance X-Windows (Motif-compliant) user interface widget for displaying images. It handles all aspects of low-level image display. The fully Motif-compliant image display widget handles the following tasks:

- Image display, including dithering as needed
- Zoom
- Pan
- Stretch (contrast enhancement, via lookup table)
- Display of single-band or color data
- Display of non-byte data (ints, floats)
- Pseudocolor display
- Full overlay support (drawing graphics on image)
- Mouse-based panning
- Cursor handling, shaping, and planting (disconnecting cursor from mouse)
- Support for all user interaction events (passed to application)
- Background loading and display of images (doesn't freeze the GUI)
- Tiling of images.

It does not read images directly, so it can work with any image file format. It is the application's responsibility to read the image and supply it to XvicImage. The xvd and tp programs (part of the VICAR image processing package) are dependent on XvicImage for their operation.

*This work was done by Robert G. Deen of Caltech for NASA's Jet Propulsion Laboratory. For more information, contact [iaoffice@jpl.nasa.gov](mailto:iaoffice@jpl.nasa.gov).*

*This software is available for commercial licensing. Please contact Daniel Broderick of the California Institute of Technology at [danielb@caltech.edu](mailto:danielb@caltech.edu). Refer to NPO-46922.*



## Binary-Signal Recovery

**Application areas include information technology and telemetry.**

*John H. Glenn Research Center, Cleveland, Ohio*

Binary communication through long cables, opto-isolators, isolating transformers, or repeaters can become distorted in characteristic ways. The usual solution is to slow the communication rate, change to a different method, or improve the communication media. It would help if the characteristic distortions could be accommodated at the receiving end to ease the communication problem. The distortions come from loss of the high-frequency content, which adds slopes to the transitions from ones to zeroes and zeroes to ones. This weakens the definition of the ones and zeroes in the time domain. The other major distortion is the reduction of low frequency, which causes the voltage that defines the ones or zeroes to drift out of recognizable range.

This development describes a method for recovering a binary data stream from a signal that has been subjected to a loss of both higher-frequency content and low-frequency content that is essential to define the difference between ones and zeroes. The method makes use of the fre-

quency structure of the waveform created by the data stream, and then enhances the characteristics related to the data to reconstruct the binary switching pattern.

A major issue is simplicity. The approach taken here is to take the first derivative of the signal and then feed it to a hysteresis switch. This is equivalent in practice to using a non-resonant band pass filter feeding a Schmitt trigger. Obviously, the derivative signal needs to be offset to halfway between the thresholds of the hysteresis switch, and amplified so that the derivatives reliably exceed the thresholds.

A transition from a zero to a one is the most substantial, fastest plus movement of voltage, and therefore will create the largest plus first derivative pulse. Since the quiet state of the derivative is sitting between the hysteresis thresholds, the plus pulse exceeds the plus threshold, switching the hysteresis switch plus, which re-establishes the data zero to one transition, except now at the logic levels of the receiving circuit. Similarly, a tran-

sition from a one to a zero will be the most substantial and fastest minus movement of voltage and therefore will create the largest minus first derivative pulse. The minus pulse exceeds the minus threshold, switching the hysteresis switch minus, which re-establishes the data one to zero transition.

This innovation has a large increase in tolerance for the degradation of the binary pattern of ones and zeroes, and can reject the introduction of noise in the form of low frequencies that can cause the voltage pattern to drift up or down, and also higher frequencies that are beyond the recognizable content in the binary transitions.

*This work was done by Elmer L. Griebeler of Glenn Research Center. Further information is contained in a TSP (see page 1).*

*Inquiries concerning rights for the commercial use of this invention should be addressed to NASA Glenn Research Center, Innovative Partnerships Office, Attn: Steven Fedor, Mail Stop 4-8, 21000 Brookpark Road, Cleveland, Ohio 44135. Refer to LEW-18576-1.*

## Volumetric 3D Display System With Static Screen

**This static glass cube display could enable 3D virtual reality environments that eliminate the need for goggles or helmets.**

*Goddard Space Flight Center, Greenbelt, Maryland*

Current display technology has relied on flat, 2D screens that cannot truly convey the third dimension of visual information: depth. In contrast to conventional visualization that is primarily based on 2D flat screens, the volumetric 3D display possesses a true 3D display volume, and places physically each 3D voxel in displayed 3D images at the true 3D ( $x,y,z$ ) spatial position. Each voxel, analogous to a pixel in a 2D image, emits light from that position to form a real 3D image in the eyes of the viewers. Such true volumetric 3D display technology provides both physiological (accommodation, convergence, binocular disparity, and motion parallax) and

psychological (image size, linear perspective, shading, brightness, etc.) depth cues to human visual systems to help in the perception of 3D objects. In a volumetric 3D display, viewers can watch the displayed 3D images from a completely 360° view without using any special eyewear. The volumetric 3D display techniques may lead to a quantum leap in information display technology and can dramatically change the ways humans interact with computers, which can lead to significant improvements in the efficiency of learning and knowledge management processes.

Within a block of glass, a large amount of tiny dots of voxels are cre-

ated by using a recently available machining technique called laser subsurface engraving (LSE). The LSE is able to produce tiny physical crack points (as small as 0.05 mm in diameter) at any ( $x,y,z$ ) location within the cube of transparent material. The crack dots, when illuminated by a light source, scatter the light around and form visible voxels within the 3D volume. The locations of these tiny voxels are strategically determined such that each can be illuminated by a light ray from a high-resolution digital mirror device (DMD) light engine. The distribution of these voxels occupies the full display volume within the static 3D glass screen. This design

eliminates any moving screen seen in previous approaches, so there is no image jitter, and has an inherent parallel mechanism for 3D voxel addressing.

High spatial resolution is possible with a full color display being easy to implement. The system is low-cost and low-maintenance.

*This work was done by Jason Geng of Xigen LLC for Goddard Space Flight Center. Further information is contained in a TSP (see page 1). GSC-15606-1*

---

## MMIC Replacement for Gunn Diode Oscillators

*Goddard Space Flight Center, Greenbelt, Maryland*

An all-solid-state replacement for high-frequency Gunn diode oscillators (GDOs) has been proposed for use in NASA's millimeter- and submillimeter-wave sensing instruments. Highly developed microwave oscillators are used to achieve a low-noise and highly stable reference signal in the 10–40-GHz band. Compact amplifiers and high-power frequency multipliers extend the signal to the 100–500-GHz band with minimal added phase noise and output power sufficient for NASA missions.

This technology can achieve improved output power and frequency

agility, while maintaining phase noise and stability comparable to other GDOs. Additional developments of the technology include: a frequency quadrupler to 145 GHz with 18 percent efficiency and 15 percent fixed tuned bandwidth; frequency doublers featuring 124, 240, and 480 GHz; an integrated 874-GHz subharmonic mixer with a mixer noise temperature of 3,000 K DSB (double sideband) and mixer conversion loss of 11.8 dB DSB; a high-efficiency frequency tripler design with peak output power of 23 mW and 14

mW, and efficiency of 16 and 13 percent, respectively; millimeter-wave integrated circuit (MMIC) power amplifiers to the 30–40 GHz band with high DC power efficiency; and an 874-GHz radiometer suitable for airborne observation with state-of-the-art sensitivity at room temperature and less than 5 W of total power consumption.

*This work was done by Thomas W. Crowe and David Porterfield of Virginia Diodes Inc. for Goddard Space Flight Center. Further information is contained in a TSP (see page 1).GSC-15630-1*

---

## Feature Acquisition With Imbalanced Training Data

*NASA's Jet Propulsion Laboratory, Pasadena, California*

This work considers cost-sensitive feature acquisition that attempts to classify a candidate datapoint from incomplete information. In this task, an agent acquires features of the datapoint using one or more costly diagnostic tests, and eventually ascribes a classification label. A cost function describes both the penalties for feature acquisition, as well as misclassification errors.

A common solution is a Cost Sensitive Decision Tree (CSDT), a branching sequence of tests with features acquired at interior decision points and class assignment at the leaves. CSDT's can incorporate a wide range of diagnostic tests and can reflect arbitrary cost structures. They are particularly useful for online

applications due to their low computational overhead.

In this innovation, CSDT's are applied to cost-sensitive feature acquisition where the goal is to recognize very rare or unique phenomena in real time. Example applications from this domain include four areas. In stream processing, one seeks unique events in a real time data stream that is too large to store. In fault protection, a system must adapt quickly to react to anticipated errors by triggering repair activities or follow-up diagnostics. With real-time sensor networks, one seeks to classify unique, new events as they occur. With observational sciences, a new generation of instrumentation seeks unique

events through online analysis of large observational datasets.

This work presents a solution based on transfer learning principles that permits principled CSDT learning while exploiting any prior knowledge of the designer to correct both between-class and within-class imbalance. Training examples are adaptively reweighted based on a decomposition of the data attributes. The result is a new, nonparametric representation that matches the anticipated attribute distribution for the target events.

*This work was done by David R. Thompson, Kiri L. Wagstaff, Walid A. Majid, and Dayton L. Jones of Caltech for NASA's Jet Propulsion Laboratory. For more information, contact iaoffice@jpl.nasa.gov. NPO-47562*



### Mount Protects Thin-Walled Glass or Ceramic Tubes From Large Thermal and Vibration Loads

Low-stress, low-profile mounts were developed for photomultiplier tubes for imaging systems, biological sensing, and atmospheric sensing.

*Goddard Space Flight Center, Greenbelt, Maryland*

The design allows for the low-stress mounting of fragile objects, like thin walled glass, by using particular ways of compensating, isolating, or releasing the coefficient of thermal expansion (CTE) differences between the mounted object and the mount itself. This mount profile is lower than true full kinematic mounting. Also, this approach enables accurate positioning of the component for electrical and optical interfaces. It avoids the higher and unpredictable stress issues that often result from “potting” the object. The mount has been built and tested to space-flight specifications, and has been used for fiber-optic, optical, and electrical interfaces for a space-flight mission.

This mount design is often metal and is slightly larger than the object to be mounted. The objects are optical or optical/electrical, and optical and/or electrical interfaces are required from the top and bottom. This requires the mount to be open at both ends, and for the object’s position to be controlled. Thin inside inserts at the top and bot-

tom contact the housing at defined lips, or edges, and hold the fragile object in the mount. The inserts can be customized to mimic the outer surface of the object, which further reduces stress. The inserts have the opposite CTE of the housing material, partially compensating for the CTE difference that causes thermal stress. A spring washer is inserted at one end to compensate for more CTE difference and to hold the object against the location edge of the mount for any optical position requirements. The spring also ensures that any fiber-optic or optic interface, which often requires some pressure to ensure a good interface, does not overstress the fragile object. The insert thickness, material, and spring washer size can be traded against each other to optimize the mount and stresses for various thermal and vibration load ranges and other mounting requirements.

The alternate design uses two separate, unique features to reduce stress and hold the object. A release agent is

applied to the inside surface of the mount just before the binding potting material is injected in the mount. This prevents the potting material from bonding to the mount, and thus prevents stress from being applied, at very low temperatures, to the fragile object being mounted. The potting material mixing and curing is temperature- and humidity-controlled. The mount has radial grooves cut in it that the potting material fills, thus controlling the vertical position of the mounted object. The design can easily be used for long and thin objects, short and wide objects, and any shape in between. The design’s advantages are amplified for long and thin fragile objects. The general testing range was  $-45$  to  $+45$  °C, but multiple mounts were successfully tested down to  $-60$  and up to  $50$  °C and the design can be adjusted for larger ranges.

*This work was done by Michael Amato, Stephen Schmidt, and James Marsh of Goddard Space Flight Center and Kevin Dahya of ATK. Further information is contained in a TSP (see page 1). GSC-15546-1*

### Carbon Nanotube-Based Structural Health Monitoring Sensors

*Langley Research Center, Hampton, Virginia*

Carbon nanotube (CNT)-based sensors for structural health monitoring (SHM) can be embedded in structures of all geometries to monitor conditions both inside and at the surface of the structure to continuously sense changes. These CNTs can be manipulated into specific orientations to create small, powerful, and flexible sensors. One of the sensors is a highly flexible sensor for crack growth detection and strain field mapping that features a very dense and highly ordered array of single-walled CNTs.

CNT structural health sensors can be mass-produced, are inexpensive, can be packaged in small sizes ( $0.5$  micron<sup>2</sup>), re-

quire less power than electronic or piezoelectric transducers, and produce less waste heat per square centimeter than electronic or piezoelectric transducers.

Chemically functionalized lithographic patterns are used to deposit and align the CNTs onto metallic electrodes. This method consistently produces aligned CNTs in the defined locations. Using photo- and electron-beam lithography, simple Cr/Au thin-film circuits are patterned onto oxidized silicon substrates. The samples are then re-patterned with a CNT-attracting, self-assembled monolayer of 3-aminopropyltriethoxysilane (APTES) to delineate the desired CNT

locations between electrodes. During the deposition of the solution-suspended single-wall CNTs, the application of an electric field to the metallic contacts causes alignment of the CNTs along the field direction. This innovation is a prime candidate for smart skin technologies with applications ranging from military, to aerospace, to private industry.

*This work was done by Russell Wincheski and Jeffrey Jordan of Langley Research Center; Donald Oglesby, Anthony Watkins, and JoAnne Patry of Swales Aerospace; Jan Smits of Lockheed Martin; and Phillip Williams of National Research Council. Further information is contained in a TSP (see page 1). LAR-16475-1*





### ⚙️ **Wireless Inductive Power Device Suppresses Blade Vibrations**

**The aerospace and electric power generation industries could benefit from this technology.**

*John H. Glenn Research Center, Cleveland, Ohio*

Vibration in turbomachinery can cause blade failures and leads to the use of heavier, thicker blades that result in lower aerodynamic efficiency and increased noise. Metal and/or composite fatigue in the blades of jet engines has resulted in blade destruction and loss of lives. Techniques for suppressing low-frequency blade vibration, such as “tuned circuit resistive dissipation of vibratory energy,” or simply “passive damping,” can require electronics incorporating coils of unwieldy dimensions and adding unwanted weight to the rotor. Other approaches, using vibration-dampening devices or damping material, could add undesirable weight to the blades or hub, making them less efficient.

A wireless inductive power device (WIPD) was designed, fabricated, and developed for use in the NASA Glenn’s “Dynamic Spin Rig” (DSR) facility. The DSR is used to simulate the functionality of turbomachinery. The relatively small and lightweight device [10 lb (≈4.5 kg)] replaces the existing venerable and bulky slip-ring. The goal is the eventual integration of this technology into actual turbomachinery such as jet engines or electric power generators, wherein the device will facilitate the suppression of potentially

destructive vibrations in fan blades. This technology obviates slip rings, which require cooling and can prove unreliable or be problematic over time.

The WIPD consists of two parts: a remote element, which is positioned on the rotor and provides up to 100 W of electrical power to thin, lightweight piezoelectric patches strategically placed on/in fan blades; and a stationary base unit that wirelessly communicates with the remote unit. The base unit supplies inductive power, and also acts as an input and output corridor for wireless measurement, and active control command to the remote unit.

Efficient engine operation necessitates minimal disturbance to the gas flow across the turbine blades in any effort to moderate blade vibration. This innovation makes it possible to moderate vibration on or in turbomachinery blades by providing 100 W of wireless electrical power and actuation control to thin, lightweight vibration-suppressing piezoelectric patches (eight actuation and eight sensor patches in this prototype, for a total of 16 channels) positioned strategically on the surface of, or within, titanium fan blades, or embedded in composite fan blades. This approach moves significantly closer

to the ultimate integration of “active” vibration suppression technology into jet engines and other turbomachinery devices such as turbine electrical generators used in the power industry.

The novel feature of this device is in its utilization of wireless technology to simultaneously sense and actively control vibration in rotating or stationary turbomachinery blades using piezoelectric patches. In the past, wireless technology was used solely for sensing and diagnostics. This technology, however, will accomplish much more, in terms of simultaneously sensing, suppressing blade vibration, and making it possible for detailed study of vibration impact in turbomachinery blades.

*This work was done by Carlos R. Morrison, Andrew J. Provenza, Benjamin B. Choi, Milind A. Bakhle, James B. Min, George L. Stefko, Kirsten P. Duffy of Glenn Research Center and John Kussmann of MESA Systems Co. and Alan J. Fougere of D-2 Inc. Further information is contained in a TSP (see page 1).*

*Inquiries concerning rights for the commercial use of this invention should be addressed to NASA Glenn Research Center, Innovative Partnerships Office, Attn: Steven Fedor, Mail Stop 4-8, 21000 Brookpark Road, Cleveland, Ohio 44135. Refer to LEW-18601-1.*

### ⚙️ **Safe, Advanced, Adaptable Isolation System Eliminates the Need for Critical Lifts**

**Inflatable isolators are integrated into an aircraft jacking system.**

*Dryden Flight Research Center, Edwards, California*

The Starr Soft Support isolation system incorporates an automatically reconfigurable aircraft jack into NASA’s existing 1-Hertz isolators. This enables an aircraft to float in mid-air without the need for a critical lift during ground vibration testing (GVT), significantly reducing testing risk, time, and costs. Currently incorporating the most advanced technology available, the 60,000-pound-capacity (27-metric-ton) isolation system

is used for weight and measurement tests, control-surface free-play tests, and structural mode interaction tests without the need for any major reconfiguration, often saving days of time and significantly reducing labor costs.

The Starr Soft Support isolation system consists of an aircraft-jacking device with three jacking points, each of which has an individual motor and accommodates up to 20,000 pounds (9 metric tons) for a

total 60,000-pound (27-metric-ton) capacity. The system can be transported to the aircraft by forklift and placed at its jacking points using a pallet jack. The motors power the electric actuators, raising the aircraft above the ground until the landing gear can retract.

Inflatable isolators then deploy, enabling the aircraft to float in mid-air, simulating a 1-Hertz free-free boundary condition. Inflatable isolators have been in

use at NASA for years, enabling aircraft to literally float unsupported for highly accurate GVT. These isolators must be placed underneath the aircraft for this to occur. Traditionally, this is achieved by a “critical lift” — a high-risk procedure in which a crane and flexible cord system are used to lift the aircraft. In contrast, the Starr Soft Support isolation system eliminates the need for critical lift by integrating the inflatable isolators into an

aircraft jacking system. The system maintains vertical and horizontal isolating capabilities. The aircraft can be rolled onto the system, jacked up, and then the isolators can be inflated and positioned without any personnel needing to work underneath the aircraft. Also, the system accommodates changes in aircraft configuration, automatically adapting to changes in mass, and it can adjust the height of the isolators in one basic setup.

Dryden personnel used the Starr Soft Support system to successfully perform a GVT on an F-15 being structurally modified by Gulfstream, Dryden’s Gulfstream III used for science research and the crew exploration module and adaptor cone assembly.

*This work was done by Starr Ginn of Dryden Flight Research Center. Further information is contained in a TSP (see page 1). DRC-009-042*

---

## **Anti-Rotation Device Releasable by Insertion of a Tool**

*Lyndon B. Johnson Space Center, Houston, Texas*

A drive mechanism enables a socket-type wrench to rotate a shaft and prevents accidental rotation of the shaft when the wrench is not coupled to the shaft. In the original intended application, the shaft would be part of an attachment mechanism on a spacecraft, and the purpose to be served by the drive is to prevent back-driving of the shaft by launch vibrations while enabling an astronaut equipped with the appropriate wrench to actuate the shaft while in orbit. The design could

also be adapted to terrestrial applications in which it is necessary to prevent rotational back-driving. The mechanism includes a gear near the tip of the shaft, and a drive nut that constitutes the tip of the shaft. The gear and drive nut are positioned in a recess in a housing. The recess is sized to receive the wrench socket that mates with the drive nut. Also contained in the housing are four linkages that include pins that are spring-loaded into engagement with the gear to prevent

rotation of the shaft. When the wrench socket is inserted in the recess, it pushes on the linkages in such a manner as to disengage the pins from the gear.

*This work was done by Harry K. Warden and Terro J. Jenkins of The Boeing Co. for Johnson Space Center. For further information, contact the Johnson Commercial Technology Office at (281) 483-3809.*

*The Boeing Co. has requested permission to assert copyright for technical data and drawings. MSC-23396-1*

---

## **A Magnetically Coupled Cryogenic Pump**

**A proof of concept pump is successful.**

*John F. Kennedy Space Center, Florida*

Historically, cryogenic pumps used for propellant loading at Kennedy Space Center (KSC) and other NASA Centers have a bellows mechanical seal and oil bath ball bearings, both of which can be problematic and require high maintenance. Because of the extremely low temperatures, the mechanical seals are made of special materials and design, have wearing surfaces, are subject to improper installation, and commonly are a potential leak path. The ball bearings are non-precision bearings [ABEC-1 (Annular Bearing Engineering Council)] and are lubricated using LOX compatible oil. This oil is compatible with the propellant to prevent explosions, but does not have good lubricating properties. Due to the poor lubricity, it has been a goal of the KSC cryogenics community for the last 15 years to develop a magnetically coupled pump, which would eliminate these two potential issues. A number of projects have been attempted, but none of the pumps was a success.

An off-the-shelf magnetically coupled pump (typically used with corrosive fluids) was procured that has been used for hypergolic service at KSC. The KSC Cryogenics Test Lab (CTL) operated the pump in cryogenic LN<sub>2</sub> “as received” to determine a baseline for modifications required. The pump bushing, bearings, and thrust rings failed, and the pump would not flow liquid (this is a typical failure mode that was experienced in the previous attempts).

Using the knowledge gained over the years designing and building cryogenic pumps, the CTL determined alternative materials that would be suitable for use under the pump design conditions. The CTL procured alternative materials for the bearings (bronze, aluminum bronze, and glass filled PTFE) and machined new bearing bushings, sleeves, and thrust rings. The designed clearances among the bushings, sleeves, thrust rings, case, and case cover were altered once again using experience gained from previous cryogenic

pump rebuilds and designs. The alternative material parts were assembled into the pump, and the pump was successfully operated meeting all expected operating parameters.

Unique pump sub-assembly parts were designed and manufactured by the CTL using specialized materials determined to be superior for cryogenic thermal applications under the pump design conditions. This work is a proof-of-concept/proof-of-operation of the pump only. Other known internal design modifications to the pump should be accomplished for the long-term use of the pump. An upscaled version of this pump, which is under development and testing at the CTL, can be used either for current or future vehicle loading or for vehicle replenishment. Scaling of this pump can be easily accomplished.

*This work was done by Walter Hatfield and Kevin Jumper of John F. Kennedy Space Center. Further information is contained in a TSP (see page 1). KSC-13434*

## Single Piezo-Actuator Rotary-Hammering Drill

The minimal number of parts in this drill increases reliability and eliminates potential failure points.

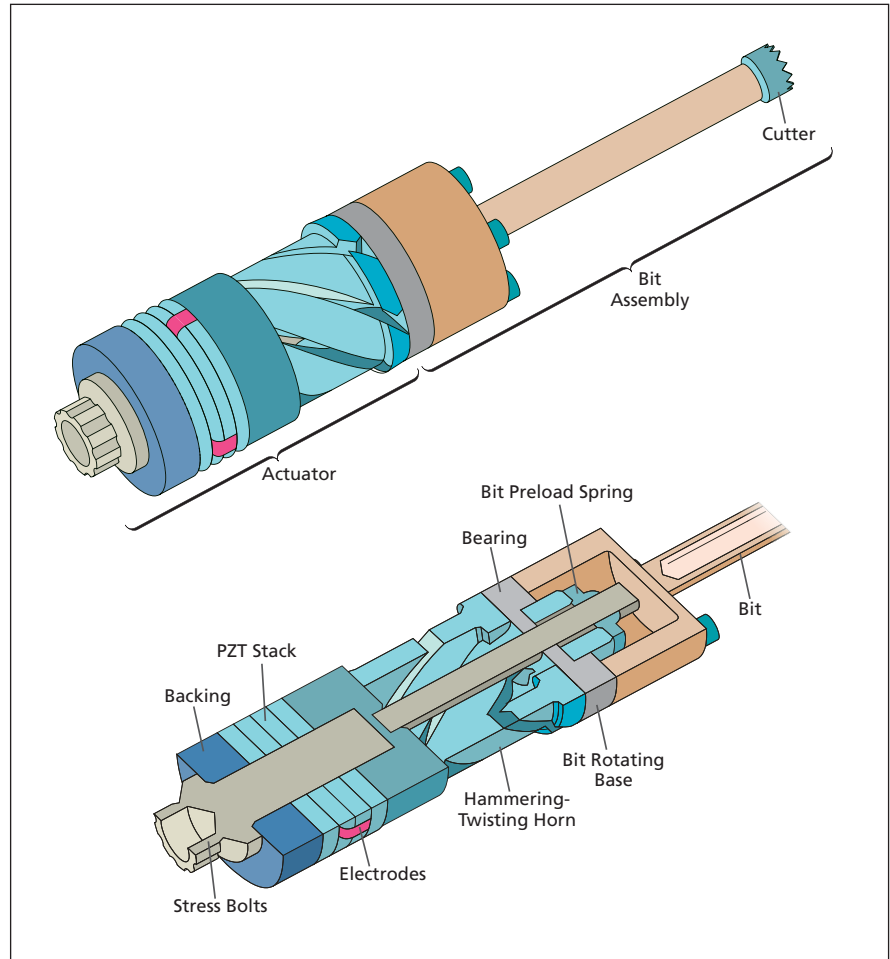
NASA's Jet Propulsion Laboratory, Pasadena, California

This innovation comprises a compact drill that uses low-axial preload, via vibrations, that fractures the rock under the bit kerf, and rotates the bit to remove the powdered cuttings while augmenting the rock fracture via shear forces. The vibrations "fluidize" the powdered cuttings inside the flutes around the bit, reducing the friction with the auger surface. These combined actions reduce the consumed power and the heating of the drilled medium, helping to preserve the pristine content of the produced samples.

The drill consists of an actuator that simultaneously impacts and rotates the bit by applying force and torque via a single piezoelectric stack actuator without the need for a gearbox or lever mechanism. This reduces the development/fabrication cost and complexity.

The piezoelectric actuator impacts the surface and generates shear forces, fragmenting the drilled medium directly under the bit kerf by exceeding the tensile and/or shear strength of the struck surface. The percussive impact action of the actuator leads to penetration of the medium by producing a zone of finely crushed rock directly underneath the struck location. This fracturing process is highly enhanced by the shear forces from the rotation and twisting action. To remove the formed cuttings, the bit is constructed with an auger on its internal or external surface. One of the problems with pure hammering is that, as the teeth become embedded in the sample, the drilling efficiency drops unless the teeth are moved away from the specific footprint location. By rotating the teeth, they are moved to areas that were not fragmented, and thus the rock fracturing is enhanced via shear forces. The shear motion creates ripping or chiseling action to produce larger fragments to increase the drilling efficiency, and to reduce the required power.

The actuator of the drill consists of a piezoelectric stack that vibrates the horn. The stack is compressed by a bolt between the backing and the horn in order to prevent it from being subjected to tensile stress that will cause it to fail. The



Cross-section and solid isometric views of the **Single Piezo-Actuator Rotary-Hammering Drill**. The bit is interfaced with the horn via a bit rotating base and is bolted to the horn via a bearing and preload spring.

backing is intended to transfer the generated mechanical vibrations towards the horn. In order to cause rotation, the horn is configured asymmetrically with helical segments and, upon impacting the bit, it introduces longitudinal along the axis of the actuator and tangential force causing twisting action that rotates the bit. The longitudinal component of the vibrations of the stack introduces percussion impulses between the bit and the rock to fracture it when the ultimate strain is exceeded under the bit.

*This work was done by Stewart Sherrit, Xiqi Bao, Mircea Badescu, and Yoseph Bar-Cohen of Caltech for NASA's Jet Propulsion*

*Laboratory. Further information is contained in a TSP (see page 1).*

*In accordance with Public Law 96-517, the contractor has elected to retain title to this invention. Inquiries concerning rights for its commercial use should be addressed to:*

*Innovative Technology Assets Management*

*JPL*

*Mail Stop 202-233*

*4800 Oak Grove Drive*

*Pasadena, CA 91109-8099*

*E-mail: iaoffice@jpl.nasa.gov*

*Refer to NPO-47216, volume and number of this NASA Tech Briefs issue, and the page number.*





## Fire-Retardant Polymeric Additives

**Mechanical properties are retained or even enhanced.**

*John F. Kennedy Space Center, Florida*

Polyhydroxyamide (PHA) and polymethoxyamide (PMeOA) are fire-retardant (FR) thermoplastic polymers and have been found to be useful as an additive for imparting fire retardant properties to other compatible, thermoplastic polymers (including some elastomers). Examples of compatible flammable polymers include nylons, polyesters, and acrylics. Unlike most prior additives, PHA and PMeOA do not appreciably degrade the mechanical properties of the matrix polymer; indeed, in some cases, mechanical properties are enhanced. Also, unlike some prior additives, PHA and PMeOA do not decompose into large amounts of corrosive or toxic compounds during combustion and can be processed at elevated temperatures.

PMeOA derivative formulations were synthesized and used as an FR additive in the fabrication of polyamide (PA) and

polystyrene (PS) composites with notable reduction (>30 percent for PS) in peak heat release rates compared to the neat polymer as measured by a Cone Calorimeter (ASTM E1354). Synergistic effects were noted with nanosilica composites. These nanosilica composites had more than 50-percent reduction in peak heat release rates.

In a typical application, a flammable thermoplastic, thermoplastic blend, or elastomer that one seeks to render flame-retardant is first dry-mixed with PHA or PMeOA or derivative thereof. The proportion of PHA or PMeOA or derivative in the mixture is typically chosen to lie between 1 and 20 weight percent. The dry blend can then be melt-extruded. The extruded polymer blend can further be extruded and/or molded into fibers, pipes, or any other of a variety of objects that may be required to be fire-retardant.

The physical and chemical mechanisms which impart flame retardancy of the additive include inhibiting free-radical oxidation in the vapor phase, preventing vaporization of fuel (the polymer), and cooling through the formation of chemical bonds in either the vapor or the condensed phase. Under thermal stress, the cyclic hydroxyl/methoxy component forms polybenzoxazole (PBO) in a reaction that absorbs heat from its surroundings. PBO under thermal stress cross-links, forming a protective char layer, which thermally insulates the polymer. Thus, the formation of the char layer further assists to extinguish the fire by preventing vaporization of the polymeric fuel.

*This work was done by Martha K. Williams and Trent M. Smith of Kennedy Space Center. For further information, contact the Kennedy Innovative Partnerships Office at (321) 861-7158. KSC-12697*

## Catalytic Generation of Lift Gases for Balloons

**Relatively lightweight, low-power gas generators are based on methanol reforming.**

*Goddard Space Flight Center, Greenbelt, Maryland*

A lift-gas cracker (LGC) is an apparatus that generates a low-molecular-weight gas (mostly hydrogen with smaller amounts of carbon monoxide and/or carbon dioxide) at low gauge pressure by methanol reforming. LGCs are undergoing development for use as sources of buoyant gases for filling zero-gauge-pressure meteorological and scientific balloons in remote locations where heavy, high-pressure helium cylinders are not readily available. LGCs could also be used aboard large, zero-gauge-pressure, stratospheric research balloons to extend the duration of flight.

Methanol reforming has been investigated as a means of generating hydrogen for fuel cells. Although the product-gas specifications, process-stream, and control requirements for fuel-cell applications differ from those of lift-gas applications, the underlying methanol-re-

forming principle is the same for both classes of applications, and some of the heat-exchange and catalyst design requirements from fuel-cell applications are adaptable to lift-gas applications.

In the methanol reforming reactor that lies at the heart of an LGC, methanol is catalytically cracked to carbon monoxide and hydrogen in an endothermic reaction, typically at a temperature in the approximate range of 250 to 350 °C and at a pressure that can lie in a range from somewhat below to somewhat above standard sea-level atmospheric pressure. A small portion of the methanol feed is diverted to a low-pressure combustor to provide the heat for the endothermic reforming reaction and maintain the reactor at the reaction temperature.

When the feedstock is pure methanol, the overall chemical reaction is  $\text{CH}_3\text{OH} \rightarrow \text{CO} + 2\text{H}_2$ . In a steam-reforming vari-

ant, the feedstock is a mixture of methanol and steam, typically comprising equal numbers of methanol and water molecules, in which case the overall chemical reaction is  $\text{CH}_3\text{OH} + \text{H}_2\text{O} \rightarrow \text{CO}_2 + 3\text{H}_2$ . The optimum choice of temperature, pressure, and catalyst depends on details of the specific application. The exact formulations of methanol-reforming catalysts are proprietary; what is known is that most of them include copper oxide and zinc oxide on alumina supports.

The only consumables needed for the methanol-reforming process in an LGC, other than methanol, are air and a small amount of electrical power for an air blower and for instrumentation. In principle, an apparatus that generates hydrogen by electrolysis of water could be used as an alternative to an LGC, but an electrolytic apparatus would be less ad-

	Lift-Gas Cracker	Electrolytic Generator
Mass, kg	<100	>2,000
Area, m <sup>2</sup>	<1	>4
Electrical Power, kW	<0.5	≈100 (From Generator)
Fuel, Grams per Standard Liter of Gas	0.1	1.4
Methanol, Grams per Standard Liter of Gas	0.35	0
Water, Grams per Standard Liter of Gas	0.2	0.8
Cost, Dollars (at 2003 Prices)	<\$10,000	>\$50,000

**Selected Parameters** are presented in comparison of an LGC capable of generating hydrogen-based lift gas and an electrolytic apparatus capable of generating hydrogen — both at a rate of 100 standard liters per minute.

vantageous in several ways: As shown by example in the table, relative to an electrolytic apparatus capable of producing hydrogen at a given rate, an LGC capable of producing hydrogen-based lift gas at the same rate is much less massive and requires much less electrical power and

much less fuel. Moreover, the LGC is more reliable and robust.

As contemplated for use in extending the duration of flight of a high-altitude balloon, an LGC would provide the lift gas for an auxiliary buoyancy-control balloon separate from a main lift bal-

loon. The buoyancy-control balloon would be used to compensate for changes in buoyancy associated with diurnal/nocturnal variations in temperature. In this application, the LGC would produce the lift gas by catalytic reforming of methanol at night. During the day, some of the lift gas would be burned with atmospheric air to produce water for use as ballast. At night, the water ballast could be dropped or could be recycled to the LGC for steam reforming of methanol. In this approach, the duration of flight could be extended by a factor of as much as four, relative to a conventional approach in which ballast is dropped at night and gas is vented during the day.

*This work was done by Robert Zubrin and Mark Berggren of Pioneer Astronautics for Goddard Space Flight Center. Further information is contained in a TSP (see page 1). GSC-14792-1*

## Ionic Liquids to Replace Hydrazine

**Customized ionic liquids offer better safety and convenience than traditional propellants.**

*Dryden Flight Research Center, Edwards, California*

A method for developing safe, easy-to-handle propellants has been developed based upon ionic liquids (ILs) or their eutectic mixtures. An IL is a binary combination of a typically organic cation and anion, which generally produces an ionic salt with a melting point below 100 °C. Many ILs have melting points near, or even below, room temperature (room temperature ionic liquids, RTILs). More importantly, a number of ILs have a positive enthalpy of formation. This means the thermal energy released during decomposition reactions makes energetic ILs ideal for use as propellants. Unlike traditional, storable propellants like hydrazine, ILs also exhibit near-zero vapor pressure. This makes them safer to handle because it eliminates hazardous inhalation — the primary pathway — as a route for toxicity in humans. Thus, ILs are ideal candidates for replacing hydrazine, which is expensive and dangerous, and poses significant handling difficulties.

Another behavior exhibited by ILs that makes them particularly attractive for replacing state-of-the-art, storable propellants is the very wide temperature range in which they remain liquid. A number of ILs have been routinely synthesized to possess glass transition points

below -60 °C (-76 °F), and decomposition temperatures in excess of 140 °C (284 °F). This behavior eliminates the stringent thermal control required for hydrazine, which freezes at 2 °C (35 °F) and boils at 113 °C (235 °F). If an IL-based propulsion system were used, spacecraft power otherwise needed to run heaters that keep hydrazine in a liquid state would be freed up for other power-hungry devices.

Another operations and safety benefit is that researchers have tremendous flexibility for dialing-in the precise behavior desired. The primary method for designing an IL for a specific task has been through careful selection of the two counterions — the cation and anion where each introduces specific properties to the binary, ionically bonded salt.

Scientists estimate there are as many as 10<sup>18</sup> possible binary ILs, which gives considerable design freedom to researchers developing new propellants. This design trade space becomes significantly larger by using eutectic mixtures of ILs. Eutectic mixtures are important because they allow for precise tailoring of decomposition thermochemistry, fluid viscosity, melting point, glass transition point, density, and virtually every other physical attribute. Recently research was completed

that began to exploit eutectic mixture ILs specifically for tailoring their behavior to optimize their use as energetic monopropellants. The goal of that effort was to develop an IL monopropellant with higher Isp (specific impulse) performance than hydrazine.

In this specific work, to date, a baseline set of energetic ILs has been identified, synthesized, and characterized. Many of the ILs in this set have excellent performance potential in their own right. In all, ten ILs were characterized for their enthalpy of formation, density, melting point, glass transition point (if applicable), and decomposition temperature. Enthalpy of formation was measured using a microcalorimeter designed specifically to test milligram amounts of energetic materials. Of the ten ILs characterized, five offer higher Isp performance than hydrazine, ranging between 10 and 113 seconds higher than the state-of-the-art propellant. To achieve this level of performance, the energetic cations 4-amino-1,2,4-triazolium and 3-amino-1,2,4-triazolium were paired with various anions in the nitrate, dicyanamide, chloride, and 3-nitro-1,2,4-triazole families. Protonation, alkylation, and butylation synthesis routes were used for creation of the different salts.

With this baseline established, future efforts will examine a large number of eutectic mixtures of these various ILs. In particular, the dicyanamide-based ILs appear to offer high performance potential, while preserving the large liquidus range so desirable for propellants. Importantly, the dicyanamide ILs did not contain any oxidizing atoms (oxygen, chlorine, fluorine), which should further enhance operational safety.

One common complaint regarding IL propellants is their high viscosity. Scientists' ability to accurately predict, *a priori*, any fluid property of a binary IL — much less a eutectic mixture of two binary ILs — is still in its infancy. However, a trend that has been seen is that large structural differences between the cation and anion seem to improve fluid properties. Therefore, one goal for future efforts will be to experiment with

different IL cores and mixtures to maximize Isp performance and density, while simultaneously reducing liquid viscosity and glass transition point.

*This work was done by Syri Koelfgen of Dryden Flight Research Center; Joe Sims, Melissa Forton, and Barry Allan of Analytical Services, Inc.; and Robin Rogers and Julia Shamshina of the University of Alabama. Further information is contained in a TSP (see page 1). DRC-010-041*

---

## Variable Emittance Electrochromics Using Ionic Electrolytes and Low Solar Absorptance Coatings

*Goddard Space Flight Center, Greenbelt, MD*

One of the last remaining technical hurdles with variable emittance devices or skins based on conducting polymer electrochromics is the high solar absorptance of their top surfaces. This high solar absorptance causes overheating of the skin when facing the Sun in space. Existing technologies such as mechanical louvers or loop heat pipes are virtually inapplicable to micro (< 20 kg) and nano (< 5 kg) spacecraft.

Novel coatings lower the solar absorption to Alpha(s) of between 0.30 and

0.46. Coupled with the emittance properties of the variable emittance skins, this lowers the surface temperature of the skins facing the Sun to between 30 and 60 °C, which is much lower than previous results of 100 °C, and is well within acceptable satellite operations ranges. The performance of this technology is better than that of current new technologies such as microelectromechanical systems (MEMS), electrostatics, and electrophoretics, especially in applications involving micro and nano spacecraft.

The coatings are deposited inside a high vacuum, layering multiple coatings onto the top surfaces of variable emittance skins. They are completely transparent in the entire relevant infrared region (about 2 to 45 microns), but highly reflective in the visible-NIR (near infrared) region of relevance to solar absorptance.

*This work was done by Prasanna Chandrasekhar of Ashwin-Ushas Corporation, Inc. for Goddard Space Flight Center. Further information is contained in a TSP (see page 1). GSC-15601-1*





## Spacecraft Radiator Freeze Protection Using a Regenerative Heat Exchanger

Heat load is reduced by more than half.

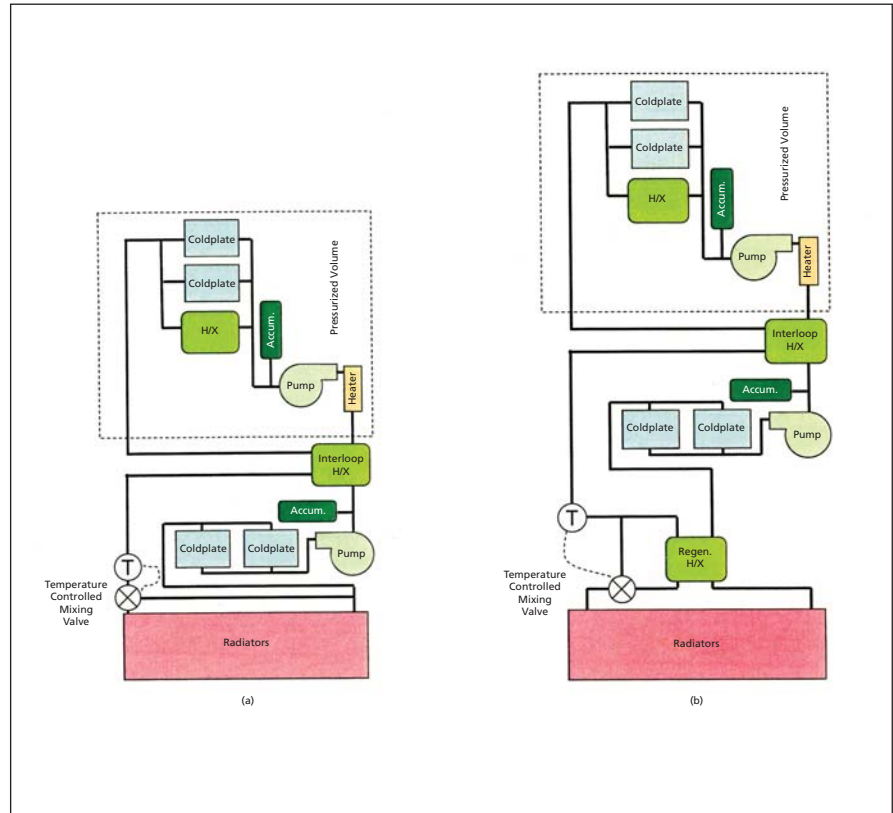
Lyndon B. Johnson Space Center, Houston, Texas

An active thermal control system architecture has been modified to include a regenerative heat exchanger (regenerator) inboard of the radiator. Rather than using a radiator bypass valve, as illustrated in (a), a regenerative heat exchanger is placed inboard of the radiators as shown in (b). A regenerator cold side bypass valve is used to set the return temperature.

During operation, the regenerator bypass flow is varied, mixing cold radiator return fluid and warm regenerator outlet fluid to maintain the system setpoint. At the lowest heat load for stable operation, the bypass flow is closed off, sending all of the flow through the regenerator. This lowers the radiator inlet temperature well below the system setpoint while maintaining full flow through the radiators.

By using a regenerator bypass flow control to maintain system setpoint, the required minimum heat load to avoid radiator freezing can be reduced by more than half compared to a radiator bypass system.

*This work was done by Eugene K. Ungar and Richard G. Schunk of Johnson Space Center. Further information is contained in a TSP (see page 1), MSC-24423-1*



(a) Active Thermal Control System with radiator bypass; (b) Active Thermal Control System Design with regenerator bypass.

## Multi-Mission Power Analysis Tool

NASA's Jet Propulsion Laboratory, Pasadena, California

Multi-Mission Power Analysis Tool (MMPAT) Version 2 simulates spacecraft power generation, use, and storage in order to support spacecraft design, mission planning, and spacecraft operations. It can simulate all major aspects of a spacecraft power subsystem. It is parametrically driven to reduce or eliminate the need for a programmer. A user-friendly GUI (graphical user interface) makes it easy to use. Multiple deployments allow use on the desktop, in batch mode, or as a callable library. It includes

detailed models of solar arrays, radioisotope thermoelectric generators, nickel-hydrogen and lithium-ion batteries, and various load types. There is built-in flexibility through user-designed state models and table-driven parameters.

MMPAT simulates a spacecraft power subsystem including the power source (solar array and/or radioisotope thermoelectric generator), bus-voltage control, secondary battery (lithium-ion or nickel-hydrogen), thermostatic heaters, and power-consuming equip-

ment. It handles multiple mission types including heliocentric orbiters, planetary orbiters, and surface operations. Being parametrically driven, along with its user-programmable features, MMPAT can reduce or even eliminate any need for software modifications when configuring it for a particular spacecraft. It provides multiple levels of fidelity, thereby fulfilling the vast majority of a project's power simulation needs throughout the life cycle. It can operate in a standalone mode with

a GUI, in batch mode, or as a library linked with other tools. It presently operates on Windows, Macintosh, Solaris, and Linux.

*This work was done by Eric G. Wood and Adrian M. Adamson of Caltech for NASA's Jet Propulsion Laboratory. For more information, contact [iaoffice@jpl.nasa.gov](mailto:iaoffice@jpl.nasa.gov).*

*This software is available for commercial licensing. Please contact Daniel Broderick of the California Institute of Technology at [danielb@caltech.edu](mailto:danielb@caltech.edu). Refer to NPO-47290.*



## Correction for Self-Heating When Using Thermometers as Heaters in Precision Control Applications

NASA's Jet Propulsion Laboratory, Pasadena, California

In precision control applications, thermometers have temperature-dependent electrical resistance with germanium or other semiconductor material thermistors, diodes, metal film and wire, or carbon film resistors. Because resistance readout requires excitation current flowing through the sensor, there is always ohmic heating that leads to a temperature difference between the sensing element and the monitored object.

In this work, a thermistor can be operated as a thermometer and a heater, simultaneously, by continuously measur-

ing the excitation current and the corresponding voltage. This work involves a method of temperature readout where the temperature offset due to self-heating is subtracted exactly.

The true temperature of an object is  $T_{\text{object}} = T_{\text{sensor}} - I \times V \times K$ , where  $I \times V$  (measured current times the measured voltage) is the power dissipated in the sensor, and  $K$  is the thermal resistance. Because the relation between the sensor electrical resistance and its temperature is typically not approximated well by a single simple function over a wide temperature range, and because the ther-

mal impedance is often temperature dependent, this solution is only easily implemented in hardware for thermistors mounted with small thermal resistance, and operating in a narrow range of set points. A software implementation is possible for a wider range of conditions, but a prior mapping of thermal resistance vs. temperature is needed.

*This work was done by Konstantin Penanen, Michael E. Ressler, Hyung J. Cho, and Kabyani G. Sukhatme of Caltech for NASA's Jet Propulsion Laboratory. Further information is contained in a TSP (see page 1). NPO-46894*

## Gravitational Wave Detection With Single-Laser Atom Interferometers

**This technique has applications in other gravity and inertial force measurements.**

NASA's Jet Propulsion Laboratory, Pasadena, California

A new design for a broadband detector of gravitational radiation relies on two atom interferometers separated by a distance  $L$ . In this scheme, only one arm and one laser are used for operating the two atom interferometers. The innovation here involves the fact that the atoms in the atom interferometers are not only considered as perfect test masses, but also as highly stable clocks. Atomic coherence is intrinsically stable, and can be many orders of magnitude more stable than a laser.

Consider a detector configuration with two ensembles of atoms separated by a distance  $L$ , in which only a single laser beam is used to operate them. The laser interrogates the atoms similarly to how a local oscillator laser interacts with atoms in an optical clock. The results give the phase differences between the laser and the highly coherent atomic internal oscillations. As the laser phase fluctuations enter into the responses of the two phase difference measurements at times separated by the one-way-light-

time,  $L$  (units in which the speed of light  $c = 1$ ), it can be shown that the laser phase fluctuations can be exactly cancelled (while retaining the gravitational wave signal) by applying time-delay interferometry (TDI) to the phase measurement data.

The fundamental limitation of a one-arm Doppler measurement configuration (such as that of interplanetary spacecraft tracking experiments) is determined by the frequency stability of the "clock" that defines the frequency of the electromagnetic link. The most stable clocks are presently optical atomic clocks, which have shown stabilities of about  $10^{-17}$  over 1,000-second integration time. This is accomplished by frequency-locking a highly stabilized laser to an atomic transition as an ideal passive frequency standard. The intrinsic atomic coherence is only limited by its natural lifetime. External perturbations cause additional frequency fluctuations, which may be controlled to a level of  $10^{-18}$  and lower. These considerations imply that atoms might be used directly

as ideal local reference oscillators for gravitational wave detection.

One of the key requirements in interferometric gravitational wave experiments is for the local reference frames to be as inertially free as possible. This is to reduce any non-gravitational forces and local gravitational disturbances that can cause changes in the laser phase. Ground-based interferometers achieve a high level of seismic isolation of their mirrors by using either passive or active isolation systems. Space-based detectors instead, such as LISA (Laser Interferometer Space Antenna), achieve inertial isolation by using highly sophisticated drag-free test masses. Although, in principle, one could trap atoms in such test masses, it is more practical to rely on laser-cooled atoms in ultra-high vacuum as alternative drag-free test masses, and to directly use them as reference sensors.

*This work was done by Nan Yu and Massimo Tinto of Caltech for NASA's Jet Propulsion Laboratory. For more information, contact [iaoffice@jpl.nasa.gov](mailto:iaoffice@jpl.nasa.gov). NPO-47334*

---

## Titanium Alloy Strong Back for IXO Mirror Segments

Potential applications include glancing-incidence mirrors and optics.

*Goddard Space Flight Center, Greenbelt, Maryland*

A titanium-alloy mirror-holding fixture called a strong back allows the temporary and permanent bonding of a 50° D263 glass x-ray mirror (IXO here stands for International X-ray Observatory). The strong back is used to hold and position a mirror segment so that mounting tabs may be bonded to the mirror with ultra-low distortion of the optical surface. Ti-15%Mo alloy was the material of choice for the strong back and tabs because the coefficient of thermal expansion closely matches that of the D263 glass and the material is relatively easy to machine.

This invention has the ability to transfer bonded mounting points from a temporary location on the strong back to a permanent location on the strong back with minimal distortion. Secondly, it converts a single mirror segment into a rigid body with an acceptable amount of distortion of the mirror, and then maneuvers that rigid body into optical alignment such that the mirror segment can be bonded

into a housing simulator or mirror module. Key problems are that the mirrors are 0.4-mm thick and have a very low coefficient of thermal expansion (CTE). Because the mirrors are so thin, they are very flexible and are easily distorted. When permanently bonding the mirror, the goal is to achieve a less than 1-micron distortion. Temperature deviations in the lab, which have been measured to be around 1 °C, have caused significant distortions in the mirror segment.

The Ti-15%Mo is with a CTE of 7.2 microinches/in./°C (7.2 mm/m/°C). It is 200 mm in height, 15 mm thick, has an azimuthal span of 51.5° and an internal radius of 242.50 mm. Mounting of the x-ray mirror consists of suspending the mirror segment in mid-air using two parallel strings and positioning a strong back to a location behind the mirror such that the mirror can be aligned and temporarily bonded to the strong back. Once this is accomplished, the surface map of the mirror

is re-measured. Tabs, which are used to support the mirror at the edges, are then located precisely to the edge of the mirror and then fastened to the edge of the strong back with fasteners. Epoxy is then injected through portals in the mirror tabs and allowed to cure. Once curing of the epoxy is complete, the temporary bonds at the back of the mirror are disconnected. The mirror surface is then re-measured with an interferometer and the results are compared to prior measurements.

Novel features include the near match between the D263 glass and the Ti-15%Mo. The mirror tabs allow epoxy to be injected in front of the mirror or behind the mirror. The strong back acts not only as a mirror segment transfer mechanism but also as the medium to mount the mirror into a permanent housing.

*This work was done by Glenn P. Byron and Chan Kai-Wing of Goddard Space Flight Center. Further information is contained in a TSP (see page 1). GSC-15850-1*

---

## Improved Ambient Pressure Pyroelectric Ion Source

This instrument enables ultra-sensitive detection of chemical and biological warfare agents.

*NASA's Jet Propulsion Laboratory, Pasadena, California*

The detection of volatile vapors of unknown species in a complex field environment is required in many different applications. Mass spectroscopic techniques require subsystems including an ionization unit and sample transport mechanism. All of these subsystems must have low mass, small volume, low power, and be rugged. A volatile molecular detector, an ambient pressure pyroelectric ion source (APPIS) that met these requirements, was recently reported by Caltech researchers to be used in *in situ* environments.

APPIS creates ions through temperature changes of the crystal. A change in temperature of the pyroelectric crystal creates a potential difference between the +z and -z surface. With a sufficient voltage buildup, electrical discharge occurs at the surface of the crystal and either positive or negative ions are produced depending on the crystal face.

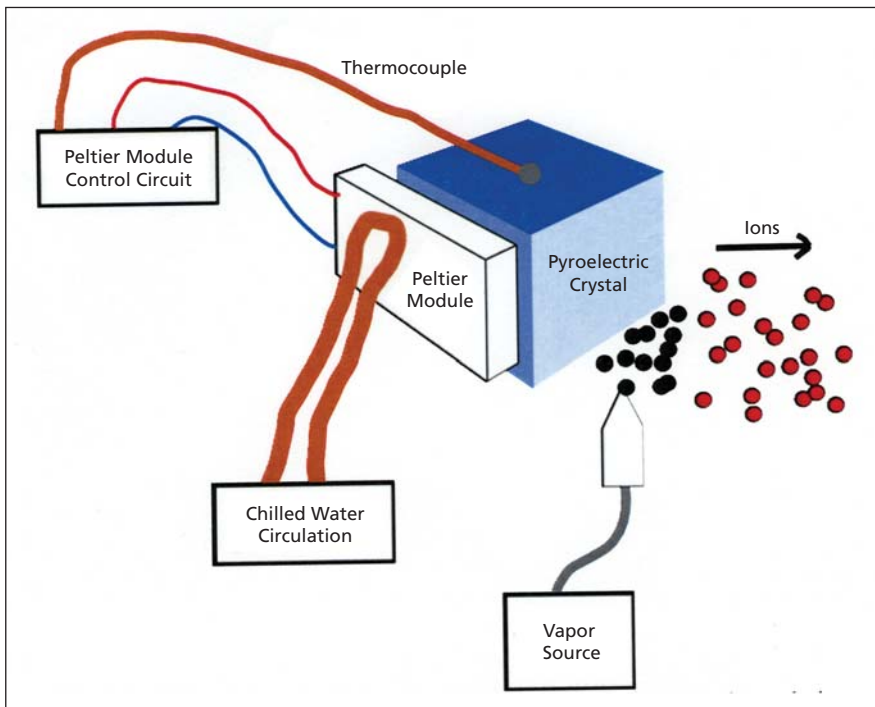
This discharge ionizes compounds on and near the surface of the crystal. If thermal cycling is applied to the pyroelectric crystal (i.e., heated and cooled repeatedly), one can obtain negative and positive ions through a thermal cycle. This process, however, creates ions at random times throughout operations and makes the source difficult to use with several detection techniques.

The improved APPIS system employs an active cooling system equipped with a feedback capability using a Peltier module to achieve better temperature control, and a heat rejection system to force-cool the crystal in order to increase the ionization efficiency of the pyroelectric crystal, on which the original APPIS source is based. In addition, the APPIS crystal housing system was completely redesigned to take advantage of the full ionization capability of the crystal source. The temperature is monitored

using a thermocouple, and a custom LabVIEW program is used to control the temperature gradient of the crystal.

A Peltier module utilizes the thermoelectric-Seebeck effect to create a temperature difference between the front and back sides of the module. If the temperature of one side of the Peltier module is heated, the other side can be cooled, depending on the polarity of the applied voltage. The system is able to provide a thermal cycling improvement compared to a conventional system by a factor of three, and can produce more uniform cooling of the crystal.

To apply thermal cycling to the crystal, two Peltier modules, one for heating and the other for cooling, are thermally bonded to the pyroelectric crystal. A chilled water pipe serves as a heat sink to prevent heating of the APPIS system. The crystal temperature is monitored with a thermocouple. The polarity of the



This schematic representation of the **APPIS System** shows the ionized vapor source coming through the analyte outlet. In a next generation of the system, the APPIS source is attached to the front end of an ambient pressure ion mobility spectrometer.

applied voltage is set by a control circuit operated by LabVIEW. When the crystal temperature heats to a threshold by one Peltier module, the other Peltier module starts cooling, and vice versa. For testing, the APPIS was mated to an ion mobility spectrometer (IMS). These two separate but fully compatible technologies are very simple to mate since both function at ambient pressures.

This APPIS-IMS system is a rugged, field-portable, low-power, and light-weight system. It has the potential for ultra-sensitive detection of molecules in both terrestrial and extraterrestrial applications such as chemical and biological warfare agents, explosives, and other harmful volatile chemical compounds, as well as organic molecule detection on Mars without use of radioactive material, complicated vacuum systems, and any consumables.

*This work was done by Luther W. Beegle, Hugh I. Kim, Isik Kanik, and Ernest K. Ryu of Caltech, and Brett Beckett of UNMS for NASA's Jet Propulsion Laboratory. For more information, contact [iaoffice@jpl.nasa.gov](mailto:iaoffice@jpl.nasa.gov). NPO-47321*





## Multi-Modal Image Registration and Matching for Localization of a Balloon on Titan

NASA's Jet Propulsion Laboratory, Pasadena, California

A solution was developed that matches visible/IR imagery aboard a balloon in Saturn's moon Titan's atmosphere to SAR (synthetic aperture radar) and visible/IR data acquired from orbit. A balloon in Titan's atmosphere must be able to localize itself autonomously both globally and with respect to local terrain. The orbital data is used to provide the balloon imagery with global context.

Due to the highly dissimilar appearance of imagery from the different types of sensors under consideration (radar, IR, visible), traditional image matching techniques based on pixel

similarity do not work. Technology pioneered by the medical imaging community has been adapted to match across sensor modalities. These techniques are driven by information content rather than appearance. While imagery of Titan's surface taken from a visible imager may appear very different from SAR imagery, there is statistical/information theoretic similarity.

The work is novel in applying mutual information (MI) to orbital vs. aerial data. There are unique challenges in this setting. Image offsets are much higher than in medical imaging, there is local distortion due to 3D terrain relief,

and the fields of regard from orbit and from the air are quite different.

Because of the large differences in image scale between an orbiter at hundreds of kilometers above the surface and a balloon at a few kilometers altitude, it is necessary to match mosaics from the balloon to single-frame orbital images. In addition to localizing the balloon, this implies the ability to generate high-resolution global maps of the surface that are correctly geo-referenced.

*This work was done by Adnan I. Ansari of Caltech for NASA's Jet Propulsion Laboratory. For more information, contact iaoffice@jpl.nasa.gov. NPO-46970*

## Entanglement in Quantum-Classical Hybrid

NASA's Jet Propulsion Laboratory, Pasadena, California

It is noted that the phenomenon of entanglement is not a prerogative of quantum systems, but also occurs in other, non-classical systems such as quantum-classical hybrids, and covers the concept of entanglement as a special type of global constraint imposed upon a broad class of dynamical systems. Application of hybrid systems for physics of life, as well as for quantum-inspired computing, has been outlined.

In representing the Schrödinger equation in the Madelung form, there is feedback from the Liouville equation to

the Hamilton-Jacobi equation in the form of the quantum potential. Preserving the same topology, the innovators replaced the quantum potential with other types of feedback, and investigated the property of these hybrid systems. A function of probability density has been introduced. Non-locality associated with a global geometrical constraint that leads to an entanglement effect was demonstrated.

Despite such a quantumlike characteristic, the hybrid can be of classical scale and all the measurements can be per-

formed classically. This new emergence of entanglement sheds light on the concept of non-locality in physics.

*This work was done by Michail Zak of Caltech for NASA's Jet Propulsion Laboratory. For more information, contact iaoffice@jpl.nasa.gov.*

*This invention is owned by NASA, and a patent application has been filed. Inquiries concerning nonexclusive or exclusive license for its commercial development should be addressed to the Patent Counsel, NASA Management Office-JPL. Refer to NPO-46213.*

## Algorithm for Autonomous Landing

NASA's Jet Propulsion Laboratory, Pasadena, California

Because of their small size, high maneuverability, and easy deployment, micro aerial vehicles (MAVs) are used for a wide variety of both civilian and military missions. One of their current drawbacks is the vast array of sensors (such as GPS, altimeter, radar, and the like) required to make a landing. Due to the MAV's small payload size, this is a major concern.

Replacing the imaging sensors with a single monocular camera is sufficient to land a MAV. By applying optical flow algorithms to images obtained from the camera, time-to-collision can be measured. This is a measurement of position and velocity (but not of absolute distance), and can avoid obstacles as well as facilitate

a landing on a flat surface given a set of initial conditions.

The key to this approach is to calculate time-to-collision based on some image on the ground. By holding the angular velocity constant, horizontal speed decreases linearly with the height, resulting in a smooth landing. Mathematical proofs show that even

with actuator saturation or modeling/measurement uncertainties, MAVs can land safely. Landings of this nature may have a higher velocity than is desirable, but this can be compensated for by a cushioning or dampening system,

or by using a system of legs to grab onto a surface.

Such a monocular camera system can increase vehicle payload size (or correspondingly reduce vehicle size), increase speed of descent, and guarantee a

safe landing by directly correlating speed to height from the ground.

*This work was done by Yoshiaki Kuwata of Caltech for NASA's Jet Propulsion Laboratory. For more information, contact [iaoffice@jpl.nasa.gov](mailto:iaoffice@jpl.nasa.gov). NPO-46549*

---

## Quantum-Classical Hybrid for Information Processing

**This innovation allows the coordination and synchronization of robots at remote distances.**

*NASA's Jet Propulsion Laboratory, Pasadena, California*

Based upon quantum-inspired entanglement in quantum-classical hybrids, a simple algorithm for instantaneous transmissions of non-intentional messages (chosen at random) to remote distances is proposed. The idea is to implement instantaneous transmission of conditional information on remote distances via a quantum-classical hybrid that preserves superposition of random solutions, while allowing one to measure its state variables using classical methods. Such a hybrid system reinforces the advantages, and minimizes the limitations, of both quantum and classical characteristics.

Consider  $n$  observers, and assume that each of them gets a copy of the system and runs it separately. Although they run identical systems, the outcomes of even synchronized runs may be different because the solutions of these systems are random. However, the global constraint must be satisfied. Therefore, if the observer #1 (the sender) made a measurement of the acceleration  $v_1$  at  $t=T$ , then the receiver, by measuring the corresponding acceleration  $v_1$  at  $t=T$ , may get a wrong value because the accelerations are random, and only their ratios are de-

terministic. Obviously, the transmission of this knowledge is instantaneous as soon as the measurements have been performed. In addition to that, the distance between the observers is irrelevant because the  $x$ -coordinate does not enter the governing equations. However, the Shannon information transmitted is zero. None of the senders can control the outcomes of their measurements because they are random. The senders cannot transmit intentional messages. Nevertheless, based on the transmitted knowledge, they can coordinate their actions based on conditional information. If the observer #1 knows his own measurements, the measurements of the others can be fully determined.

It is important to emphasize that the origin of entanglement of all the observers is the joint probability density that couples their actions. There is no centralized source, or a sender of the signal, because each receiver can become a sender as well. An observer receives a signal by performing certain measurements synchronized with the measurements of the others. This means that the signal is uniformly and simultaneously distributed over the observers in

a decentralized way. The signals transmit no intentional information that would favor one agent over another. All the sequence of signals received by different observers are not only statistically equivalent, but are also point-by-point identical. It is important to assume that each agent knows that the other agent simultaneously receives the identical signals. The sequences of the signals are true random, so that no agent could predict the next step with the probability different from those described by the density.

Under these quite general assumptions, the entangled observers-agents can perform non-trivial tasks that include transmission of conditional information from one agent to another, simple paradigm of cooperation, etc. The problem of behavior of intelligent agents correlated by identical random messages in a decentralized way has its own significance: it simulates evolutionary behavior of biological and social systems correlated only via simultaneous sensing sequences of unexpected events.

*This work was done by Michail Zak of Caltech for NASA's Jet Propulsion Laboratory. For more information, contact [iaoffice@jpl.nasa.gov](mailto:iaoffice@jpl.nasa.gov). NPO-46367*

---

## Small-Scale Dissipation in Binary-Species Transitional Mixing Layers

**This method enables cost-effective modeling for supercritical conditions prevailing in gas-turbine and liquid-rocket engines.**

*NASA's Jet Propulsion Laboratory, Pasadena, California*

Motivated by large eddy simulation (LES) modeling of supercritical turbulent flows, transitional states of databases obtained from direct numerical simulations (DNS) of binary-species supercritical temporal mixing layers were examined to understand the subgrid-scale dissipation, and its variation with filter size. Examination of the DSN-scale do-

main-averaged dissipation confirms previous findings that, out of the three modes of viscous, temperature and species-mass dissipation, the species-mass dissipation is the main contributor to the total dissipation. The results revealed that the percentage of species-mass by total dissipation is nearly invariant across species systems and initial conditions.

This dominance of the species-mass dissipation is due to high-density-gradient magnitude (HDGM) regions populating the flow under the supercritical conditions of the simulations; such regions have also been observed in fully turbulent supercritical flows. The domain average being the result of both the local values and the extent of the HDGM

regions, the expectations were that the response to filtering would vary with these flow characteristics. All filtering here is performed in the dissipation range of the Kolmogorov spectrum, at filter sizes from 4 to 16 times the DNS grid spacing. The small-scale (subgrid scale, SGS) dissipation was found by subtracting the filtered-field dissipation from the DNS-field dissipation.

In contrast to the DNS dissipation, the SGS dissipation is not necessarily positive; negative values indicate backscatter. Backscatter was shown to be spatially widespread in all modes of dissipation and in the total dissipation (25 to 60 percent of the domain). The maximum magnitude of the negative subgrid-scale dissipation was as much as 17 percent of the maximum positive subgrid-scale dissipation, indicating that, not only is backscatter spatially widespread in these flows, but it is considerable in magnitude and cannot be ig-

nored for the purposes of LES modeling. The Smagorinsky model, for example, is unsuited for modeling SGS fluxes in the LES because it cannot render backscatter. With increased filter size, there is only a modest decrease in the spatial extent of backscatter. The implication is that even at large LES grid spacing, the issue of backscatter and related SGS-flux modeling decisions are unavoidable.

As a fraction of the total dissipation, the small-scale dissipation is between 10 and 30 percent of the total dissipation for a filter size that is four times the DNS grid spacing, with all OH cases bunched at 10 percent, and the HN cases spanning 24–30 percent. A scale similarity was found in that the domain-average proportion of each small-scale dissipation mode, with respect to the total small-scale dissipation, is very similar to equivalent results at the DNS scale. With increasing filter size, the proportion of

the small-scale dissipation in the dissipation increases substantially, although not quite proportionally. When the filter size increases by four-fold, 52 percent for all OH runs, and 70 percent for HN runs, of the dissipation is contained in the subgrid-scale portion with virtually no dependence on the initial conditions of the DNS.

The indications from the dissipation analysis are that modeling efforts in LES of thermodynamically supercritical flows should be focused primarily on mass-flux effects, with temperature and viscous effects being secondary. The analysis also reveals a physical justification for scale-similarity type models, although the suitability of these will need to be confirmed in *a posteriori* studies.

*This work was done by Josette Bellan and Nora Okong'o of Caltech for NASA's Jet Propulsion Laboratory. For more information, contact iaoffice@jpl.nasa.gov. NPO-46389*

## Superpixel-Augmented Endmember Detection for Hyperspectral Images

**Hyperspectral image analysis can be used in remote sensing or industrial applications such as automated detection of manufacturing defects.**

*NASA's Jet Propulsion Laboratory, Pasadena, California*

Superpixels are homogeneous image regions comprised of several contiguous pixels. They are produced by shattering the image into contiguous, homogeneous regions that each cover between 20 and 100 image pixels. The segmentation aims for a many-to-one mapping from superpixels to image features; each image feature could contain several superpixels, but each superpixel occupies no more than one image feature. This conservative segmentation is relatively easy to automate in a robust fashion.

Superpixel processing is related to the more general idea of improving hyperspectral analysis through spatial constraints, which can recognize subtle features at or below the level of noise by exploiting the fact that their spectral signatures are found in neighboring pixels. Recent work has explored spatial constraints for endmember extraction, showing significant advantages over techniques that ignore pixels' relative positions. Methods such as AMEE (automated morphological endmember extraction) express spatial influence using fixed isometric relationships

— a local square window or Euclidean distance in pixel coordinates. In other words, two pixels' covariances are based on their spatial proximity, but are independent of their absolute location in the scene. These isometric spatial constraints are most appropriate when spectral variation is smooth and constant over the image.

Superpixels are simple to implement, efficient to compute, and are empirically effective. They can be used as a preprocessing step with any desired endmember extraction technique. Superpixels also have a solid theoretical basis in the hyperspectral linear mixing model, making them a principled approach for improving endmember extraction. Unlike existing approaches, superpixels can accommodate non-isometric covariance between image pixels (characteristic of discrete image features separated by step discontinuities). These kinds of image features are common in natural scenes.

Analysts can substitute superpixels for image pixels during endmember analysis that leverages the spatial contiguity of

scene features to enhance subtle spectral features. Superpixels define populations of image pixels that are independent samples from each image feature, permitting robust estimation of spectral properties, and reducing measurement noise in proportion to the area of the superpixel. This permits improved endmember extraction, and enables automated search for novel and constituent minerals in very noisy, hyperspatial images.

This innovation begins with a graph-based segmentation based on the work of Felzenszwalb et al., but then expands their approach to the hyperspectral image domain with a Euclidean distance metric. Then, the mean spectrum of each segment is computed, and the resulting data cloud is used as input into sequential maximum angle convex cone (SMACC) endmember extraction.

*This work was done by David R. Thompson and Rebecca Castaño of Caltech, and Martha S. Gilmore of Wesleyan University for NASA's Jet Propulsion Laboratory. For more information, contact iaoffice@jpl.nasa.gov. NPO-47358*

---

## ➤ Coding for Parallel Links To Maximize the Expected Value of Decodable Messages

**Error-correcting codes help balance throughput and reliability.**

*NASA's Jet Propulsion Laboratory, Pasadena, California*

When multiple parallel communication links are available, it is useful to consider link-utilization strategies that provide tradeoffs between reliability and throughput. Interesting cases arise when there are three or more available links. Under the model considered, the links have known probabilities of being in working order, and each link has a known capacity. The sender has a number of messages to send to the receiver. Each message has a size and a value (i.e., a worth or priority). Messages may be divided into pieces arbitrarily, and the value of each piece is proportional to its size. The goal is to choose combinations of messages to send on the links so that the expected value of the messages decodable by the receiver is maximized.

There are three parts to the innovation: (1) Applying coding to parallel links under the model; (2) Linear programming formulation for finding the optimal combinations of messages to send on the links; and (3) Algorithms for assisting in finding feasible combinations of messages, as support for the linear programming formulation.

There are similarities between this innovation and methods developed in the field of network coding. However, network coding has generally been concerned with either maximizing throughput in a fixed network, or robust communication of a fixed volume of data. In contrast, under this model, the throughput is expected to vary depending on the state of the network. Examples of error-correcting codes

that are useful under this model but which are not needed under previous models have been found.

This model can represent either a one-shot communication attempt, or a stream of communications. Under the one-shot model, message sizes and link capacities are quantities of information (e.g., measured in bits), while under the communications stream model, message sizes and link capacities are information rates (e.g., measured in bits/second).

This work has the potential to increase the value of data returned from spacecraft under certain conditions.

*This work was done by Matthew A. Klimesh and Christopher S. Chang of Caltech for NASA's Jet Propulsion Laboratory. For more information, contact [iaoffice@jpl.nasa.gov](mailto:iaoffice@jpl.nasa.gov). NPO-46593*



## Microwave Tissue Soldering for Immediate Wound Closure

**Wounds can be closed rapidly, without staples, sutures, or tapes.**

*Lyndon B. Johnson Space Center, Houston, Texas*

A novel approach for the immediate sealing of traumatic wounds is under development. A portable microwave generator and handheld antenna are used to seal wounds, binding the edges of the wound together using a biodegradable protein sealant or "solder." This method could be used for repairing wounds in emergency settings, by restoring the wound surface to its original strength within minutes. This technique could also be utilized for surgical purposes involving solid visceral organs (i.e., liver, spleen, and kidney) that currently do not respond well to ordinary surgical procedures.

A miniaturized microwave generator and a handheld antenna are used to deliver microwave energy to the protein solder, which is applied to the wound. The antenna can be of several alternative designs optimized for placement either in contact with or proximity to the protein solder covering the wound. In either case, optimization of the design includes the matching of impedances to maximize the energy delivered to the protein solder and wound at a chosen frequency. For certain applications, an antenna could be designed that would emit power only when it is in direct con-

tact with the wound.

The optimum frequency or frequencies for a specific application would depend on the required depth of penetration of the microwave energy. In fact, a computational simulation for each specific application could be performed, which would then match the characteristics of the antenna with the protein solder and tissue to best effect wound closure. An additional area of interest with potential benefit that remains to be validated is whether microwave energy can effectively kill bacteria in and around the wound. Thus, this may be an efficient method for simultaneously sterilizing and closing wounds.

Using microwave energy to seal wounds has a number of advantages over lasers, which are currently in experimental use in some hospitals. Laser tissue welding is unsuitable for emergency use because its large, bulky equipment cannot be easily moved between operating rooms, let alone relocated to field sites where emergencies often occur. In addition, this approach is highly dependent on the uniformity and thickness of the protein solder as well as the surgeon's skills. In contrast, the use of

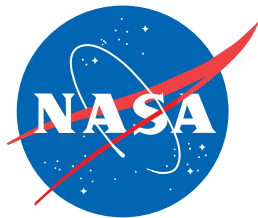
microwave energy is highly tolerant of the thickness of the protein solder, level of fluids in and around the wound, and other parameters that can adversely affect the outcome of laser welding. However, controlling the depth of penetration of the microwave energy into the wound is critical for achieving effective wound sealing without damaging the adjacent tissue. In addition, microspheres that encapsulate metallic cores could also be incorporated into the protein solder to further control the depth of penetration of the microwave energy.

*This work was performed by G. Dickey Arndt, Phong H. Ngo, Chau T. Phan, and Diane Byerly of Johnson Space Center, John Dosl of Jacobs Sverdrup, Marguerite A. Sognier of Universities Space Research Association, and Jim Carl of Advanced Electromagnetics. For further information, contact the JSC Innovation Partnerships Office at (281) 483-3809.*

*This invention is owned by NASA, and a patent application has been filed. Inquiries concerning nonexclusive or exclusive license for its commercial development should be addressed to the Patent Counsel, Johnson Space Center, (281) 483-1003. Refer to MSC-24238-1.*







National Aeronautics and  
Space Administration